Agricultural and Forest Meteorology 326 (2022) 109159

Contents lists available at ScienceDirect

Agricultural and Forest Meteorology

journal homepage: www.elsevier.com/locate/agrformet

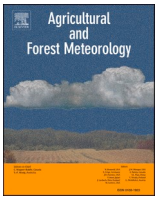

Vapour pressure deficit and solar radiation are the major drivers of transpiration in montane tropical secondary forests in eastern Madagascar

Chandra Prasad Ghimire [a,*], H.J. (Ilja) van Meerveld [b], Bob W. Zwartendijk [c,d], L. Adrian Bruijnzeel [e,f], Maafaka Ravelona [g], Jaona Lahitiana [g], Maciek W. Lubczynski [h]

[a] AgResearch, Lincoln Research Centre, Private Bag 4749, Christchurch 8140, New Zealand
[b] Department of Geography, Hydrology and Climate, University of Zurich, Winterthurerstrasse 190, 8057 Zurich, Switzerland
[c] Hydrology and Quantitative Water Management Group, Wageningen University & Research, PO Box 47, 6700 AA Wageningen, the Netherlands
[d] Research and Innovation Centre Techniek, Ontwerpen en Informatica, Inholland University of Applied Sciences, Bergerweg 200, 1817 MN Alkmaar, the Netherlands
[e] Department of Geography, King's College London, Bush House, 30 Aldwych, London WC2B 4BG, United Kingdom
[f] Institute of International Rivers and Eco-Security, Yunnan University, Kunming 650091, P. R. China
[g] Laboratoire des Radio-Isotopes, University of Antananarivo, BP 3383, Route d'Andraisoro, 101 Antananarivo, Madagascar
[h] Faculty of Geo-information and Earth Observation (ITC), University of Twente, Enschede, Hengelosestraat 99, 7514 AE Enschede, the Netherlands

ARTICLE INFO

Keywords:
Sap flow
Soil water
Stable isotopes
Transpiration
Tropical forest regeneration

ABSTRACT

Young secondary tropical forests occupy a larger area than mature forests nowadays but our understanding of their ecohydrological functioning, particularly with respect to tree water uptake, remains poor. Deep soil water uptake may make mature forests resilient to periods of water stress, but little is known in this regard for young forests with possibly less extensive root networks. We, therefore, studied sap flow dynamics for one year in two 50 m x 50 m forest plots: a young secondary forest (YSF, 5–7 years) and a semi-mature forest (SMF; 20 years) in montane eastern Madagascar. Temporal variations in the depth of water uptake were inferred from the stable isotope compositions of soil- and xylem water. Transpiration rates were low for both forest sites (265 and 462 mm y^{-1} for the YSF and SMF, respectively). Vapour pressure deficit and global radiation explained most of the variation in transpiration rates at both sites. There was little evidence of transpiration limitation by soil water, despite an extended dry season. Trees in the YSF extracted water mostly from the intermediate soil depth (30–70 cm) during the dry season. In the SMF, the depth of uptake increased as the dry season progressed for some species (*Abrahamia, Brachylaena* and *Cryptocaria*), but not for others (*Ocotea* and *Eugenia*). Although the transpiration rates are low for both forests, they are comparable to results reported for other tropical montane sites after normalising for net energy input and leaf area. Estimated evapotranspiration totals (including interception loss, understorey and litter evaporation) were 679 mm and 1063 mm y^{-1} for the YSF and SMF, respectively (42% and 61% of precipitation, respectively). These results suggest that the stage of forest regrowth affects water uptake, and thus the water balance during forest succession.

1. Introduction

The global terrestrial evaporative flux is dominated by plant transpiration (Good et al., 2015; Jasechko et al., 2013; Schlesinger and Jasechko, 2014), thereby affecting water availability and climate (Andréassian, 2004; Bonan, 2016; Ellison et al., 2017; Law et al., 2002). Given the important role of transpiration, an in-depth understanding of plant water uptake, and how it is affected by soil water availability is vital for developing effective regional and global models for the prediction of the ecological and hydrological impacts of climate- and land-cover change (Alkama and Cescatti, 2016; Bonan, 2008; Devaraju et al., 2015; Foley et al., 2007; Hu et al., 2018; Peng et al., 2014; Von Randow et al., 2019).

Forests are still being converted to agricultural land through slash-and-burn in many tropical areas (Curtis et al., 2018; Heinimann et al., 2017; Li et al., 2018). The fields are typically abandoned after a few years of cultivation because of decreases in crop yields and invasion of weeds (Styger et al., 2007; van Vliet et al., 2012). As a result, many tropical landscapes nowadays consist of a mosaic of mature forest remnants, crop land, and vegetation at different stages of regrowth, with

* Correspondence to: AgResearch Ltd Corporate Office: AgResearch Ltd, 1365 Springs Rd, Christchurch 7674, New Zealand.
E-mail address: chandra.ghimire@agresearch.co.nz (C.P. Ghimire).

https://doi.org/10.1016/j.agrformet.2022.109159
Received 5 January 2022; Received in revised form 28 August 2022; Accepted 5 September 2022
Available online 26 September 2022

(young) secondary forests often occupying a larger area than the remaining mature forest (Chazdon, 2014; FAO, 2016). However, the ecohydrological functioning of tropical secondary forests is still poorly understood (Bretfeld et al., 2018; Ghimire et al., 2018; Giambelluca, 2002; cf. Mukul and Herbohn, 2016).

Various studies have documented the changes in rainfall interception during regrowth of tropical forests (Ghimire et al., 2017; Hölscher et al., 2003; Hölscher et al., 1998; Kunert et al., 2015; Macinnis-Ng et al., 2014; Zimmermann et al., 2013), but much less is known about the corresponding changes in transpiration and the relative importance of the key factors that affect it at different successional stages (Berry et al., 2017; Bretfeld et al., 2018; cf. Kunert et al., 2015). Previous work has shown that transpiration during the first 2.5–4.5 years of lowland tropical forest succession tends to be less than that of old-growth forest (Hölscher et al., 1997; Sommer et al., 2002). There is also some evidence that transpiration rates during the intermediate growth stage (~15–25 years) may exceed those of mature forest (Giambelluca et al., 2000; von Randow et al., 2020) because the maximum stomatal conductance of early successional tropical species tend to be higher than those of late-successional ones (Juhrbandt et al., 2004; von Randow et al., 2020). Although advected energy from warmer deforested areas may have enhanced transpiration in some cases (Giambelluca et al., 2000; Giambelluca et al., 2003; Hölscher et al., 1997), similar patterns of declining transpiration rates after a peak at an intermediate age have been reported for some types of regenerating temperate broad-leaf forests (Roberts et al., 2001; Vertessy et al., 2001).

Tree transpiration and root water uptake depend on biological factors, such as species, wood anatomical properties, tree size, rooting depth, and leaf surface area, as well as environmental factors, such as available radiation, atmospheric vapour pressure deficit (VPD), wind speed, and soil water availability. For a given climatic condition, biological factors and water availability are the key determinants of transpiration (Bretfeld et al., 2018; Ghimire et al., 2018; McJannet et al., 2007; O'Grady et al., 1999). Therefore, investigating transpiration under conditions of varying water availability can provide important insights into the response of vegetation to seasonal variations in precipitation or a drying climate (Bretfeld et al., 2018; Hu et al., 2018; Nepstad et al., 2002; Schwendenmann et al., 2010).

Whether – and to what extent – reduced soil moisture availability will reduce transpiration rates during dry periods depends also on the depth of plant water uptake. The stable isotope signature (δ^2H and/or $\delta^{18}O$) of soil and xylem water can be used to determine the source of tree water use. Based on the degree of overlap in the isotopic compositions of xylem water and soil water at different depths, Amin et al. (2020) suggested that trees in seasonally dry tropical areas predominantly use water from deeper soil layers. Indeed, several studies have shown that transpiration rates were sustained or even increased during the dry season because the trees were able to access deeper soil water resources (Jackson et al., 1995; Meinzer et al., 1999; Querejeta et al., 2007; Querejeta et al., 2006; Schwendenmann et al., 2015). Trees in eastern Amazonia were similarly insensitive to dry upper-soil conditions due to their ability to access water from deeper soil layers (Oliveira et al., 2005). However, for a tropical montane forest in eastern Mexico the depth of tree water uptake became shallower as the dry season progressed due to nutrient limitations (Muñoz-Villers et al., 2018). Little information is available in this regard for secondary tropical forests at different growth stages (Pineda-García et al., 2013), although inferences of the general depth of water uptake during different seasons beneath young regrowth in Amazonia have been made based on soil water depletion observations (Sommer et al., 2003).

It is important to understand whether – and under what conditions – transpiration rates in young and older secondary forests may become limited by soil moisture deficits, and if the vegetation responds to dry conditions by changing the depth of water uptake. For example, Bretfeld et al. (2018) showed that early successional forests in Panama were more vulnerable to drought stress than late successional forest, and tentatively attributed this to a greater proportion of deep water use by the larger trees of the older forest. To better understand transpiration rates in secondary forests at different stages of succession, and how water uptake is affected by seasonal soil moisture availability, we instrumented two differently aged secondary forests in eastern Madagascar: a young secondary forest (YSF, 5–7 years old) and a semi-mature forest (SMF, ~20 years). We conducted concurrent measurements of microclimate, sap flow and soil moisture content, in combination with xylem- and soil water sampling and stable isotope analysis, over a full seasonal cycle to characterise changes in transpiration rates and depth of water uptake for selected tree species. More specifically, we address the following questions:

a) How do tree transpiration rates differ for a young- and semi-mature secondary forest?
b) What are the main drivers of transpiration for a young and semi-mature forest and is transpiration affected by soil moisture?
c) Does tree water uptake shift to deeper water sources as the dry season progresses?

2. Material and methods

2.1. Study site description

The study was conducted near Andasibe in the southern part of the Ankeniheny-Zhamena Corridor (CAZ) in eastern Madagascar (18.9°S, 48.4°E; Figure S1). The tropical monsoonal climate is characterised by two seasons: a warm, rainy season from November to April; and a cooler, dry season from May to October. Mean (± standard deviation, SD) annual precipitation measured at Andasibe (990 m a.s.l.) for the period 1983–2013 was 1625 ± 260 mm (Météo Madagascar, unpublished data). The rainy season brings about 75% of the annual total precipitation. The wettest months are January and February, which together account for 36 ± 7% of annual precipitation on average (average monthly precipitation totals of 303 ± 145 mm and 290 ± 98 mm, respectively; Météo Madagascar, unpublished data). September is the driest month with an average monthly precipitation of 35 ± 17 mm (2 ± 1% of the annual precipitation). Average monthly temperatures at Andasibe range from 15°C in July to 22°C in December (1983–2013). The average monthly relative humidity between October 2014 and November 2015 varied from 85% in October to 94% in July. Average monthly wind speeds during the same period were < 2 m s^{-1}. Further climatic information is presented in Results Section 4.1.

Long-term practicing of slash-and-burn agriculture in the area has resulted in a highly fragmented landscape that is composed of rain forest remnants, secondary forests at various stages of regrowth and young fallow vegetation on recently abandoned land, along with fire-climax grassland, scattered agricultural fields and villages (Horning & Hewson, 2017). The measurements were taken in two 50 m x 50 m forest plots: a young secondary forest (YSF, 5–7 years old) and a semi-mature forest (SMF, ~20 years old) (Table 1), located ca. 2.5 km apart. The two plots are located on fairly steep slopes (15–20°) and underlain by deeply weathered gneissic rocks. The YSF is located on a northwest-facing slope at ~ 990 m a.s.l. and the SMF on a northeast-facing slope at ~950 m a.s.l. Both the YSF and SMF stands extended beyond the 50 m x 50 m plot boundaries for another 20-100 m (depending on direction). The stands were surrounded by mixed trees and shrubs or trees of similar age as the study sites. A such, edge effects (i.e., increased diurnal amplitudes for temperature, humidity, radiation, and wind speed close to the forest edge; cf. Giambelluca et al., 2003; Kunert et al., 2015) were considered to be small or negligible. The soils have a clay (YSF) to clay-loam (SMF) texture (Table 1). Soil organic carbon content and saturated hydraulic conductivity decrease rapidly with depth at both sites (Table 1).

The evergreen YSF site was covered by lower montane rain forest before it was cut and burned for the first time in living memory for rice cultivation in 1990. It subsequently underwent three cycles of slash-and-

Table 1
Characteristics of the YSF and the SMF study plots. Average values are given with their standard deviation (±SD). Both plots were 50 m x 50 m in size.

		YSF	SMF
Elevation (m.a.s.l.)		990	950
Latitude (S)		18.9472°	18.9317°
Longitude (E)		48.3953°	48.4117°
Aspect		NW	NE
Slope		16°	18°
Basal area (m^2 ha^{-1})		6.3	35.5
Stem density (stems ha^{-1})		2133	5233
Average (±SD) canopy height* (m)		5.0 (±0.3) (n=25)	19 (±8) (n=54)
Average (±SD) DBH (cm)		6.1 (±1.3) (n=61)	9.3 (±4.0) (n=156)
Average (and range) LAI** (m^2 m^{-2})		1.83 (1.75–2.14)	3.39 (3.11–3.58)
Average (±SD) sapwood area (cm^2)		27.5 (±7.8) (n=20)	173 (±103) (n=54)
Sand/Silt/Clay (%)		23/27/50	35/26/39
Median hydraulic conductivity (mm h^{-1})	0–10 cm	981	745
	10–20 cm	27	58
	20–30 cm	1	3
Average (±SD) soil organic carbon content ***(g kg^{-1})	10 cm	38 (±4)	51 (±6)
	30 cm	23 (±7)	30 (±5)
	100 cm	2.5 (±1.2)	4.3 (±0.6)

* Determined using a Nikon Forestry Pro Laser Rangefinder.
** Determined using a Licor LAI 2000 Plant Canopy Analyzer.
*** After Razakamanarivo et al. (2017).

burn cultivation during a period of ~10 years. Several indigenous tree species were planted at the site as part of a reforestation programme in 2000, but these were rapidly out-competed by naturally regenerating *Psiadia altissima* (DC.) Drake and invasive shrubs. At the start of the measurements (October 2014), the YSF consisted mostly of *P. altissima* trees (95% of overall stem density), with native *Cassinopsis madagascariensis* Bail. and *Harungana madagascariensis* Lam. ex Poir. together occupying less than 5% of the overall stem density. The vast majority of trees were similarly sized: 85% of all stems with a diameter at breast height (DBH) ≥ 5 cm belong to the 5–7 cm diameter class, 14% to the 7–9 cm class, and 1% to the 9–11 cm class. The understorey was dominated by invasive *Rubus moluccanus* L., *Lantana camara* L. and *Clidemia hirta* (L.) D. Don, with an estimated LAI of 0.47 (Ghimire et al., 2018).

The evergreen SMF has not been cleared, burned or cultivated in living memory but was subject to illegal logging until 1995. It is now a protected forest. Many of the trees re-sprouted naturally and were thus ca. 20 years old at the time of the study. Approximately 65% of all trees with a DBH ≥ 5 cm had a diameter of 5–10 cm, while 33% had a DBH of 10–20 cm. The plot contained 72 species. The six dominant species were *Abrahamia ditimena* (H. Perrier) Randrian. & Lowry, *Brachylaena ramiflora* (DC.) Humbert, *Cryptocaria* sp., *Ocotea samosa, Eugenia* spp., and *Leptolaena* Thouars s.s., which together comprised 35% of the overall stem density. The SMF had a well-developed understorey.

2.2. Micrometeorological and soil moisture measurements

The measurements were taken between 1 October 2014 and 30 September 2015. Air temperature (T, °C) and relative humidity (RH, percentage of saturation) were measured inside a radiation shield at both sites (Skye Instruments Ltd., UK). Wind speed (m s^{-1}) was measured using an A100R digital anemometer (Vector Instruments, UK). Measurements were taken at 30 s intervals, and 10-min averages were recorded on DataHog2 loggers (Skye Instruments Ltd., UK). At the YSF, the micrometeorological measurements were made at 2 m above the forest canopy using a 7 m mast. Due to the high stem density and tall trees, it was not feasible to erect a tower above the canopy in the SMF. Therefore, measurements were made on a 10 m mast in a nearby (~100 m away) clearing.

Incident precipitation (P, mm) was measured at each site using a tipping bucket rain gauge (Rain Collector II, Davis Instruments, USA; 0.2 mm per tip) that was installed at 1 m above the soil surface. A manual rain gauge (CM1016 Skyview, UK; 10 cm orifice diameter) was used to check the data from the recording gauges.

Volumetric soil moisture contents (θ) were measured at 5, 15, 40, 75, 110 and 160 cm below the surface at each site using water content reflectometers (CS616, Campbell Scientific Ltd., USA). The 5-min data were recorded on a CR1000 data-logger (Campbell Scientific Ltd., USA). Total soil water storage (mm) was calculated for the 0–30, 30–70 and 70–160 cm depth intervals by summing the multiplication of the moisture content and the distance between the sensors within these depth intervals. We made a rough estimate of the amounts of water that is not available to plants (i.e., the residual moisture content) based on the soil water retention curves derived using the ROSETTA model (Schaap et al., 2001) and the bulk density and texture of the soil at each plot.

Incoming short-wave radiation (R_s) was measured every 30 sec at an automatic weather station located at 965 m a.s.l. in a grassland clearing (1.0 km from the SMF and 1.5 km from the YSF) using a CM6B-pyranometer (Kipp and Zonen, The Netherlands). The 5-min averages were recorded on a Campbell Scientific Ltd. CR1000 data-logger. The pyranometer was used on several occasions to measure the reflected short-wave radiation above the YSF. The resulting average albedo (0.15) was used together with the R_s as measured in the grassland clearing to compute the short-wave component of net radiation (R_n) for the YSF. It was not possible to measure the reflected short-wave radiation above the SMF due to the tall trees and uneven height of the canopy. Instead, the albedo value (0.135) for a 25-year-old tropical montane forest in northern Thailand (Giambelluca et al., 1999) was used to estimate the short-wave component of R_n for the SMF. The net long-wave radiation was estimated for both sites using a Brunt-type formula based on the locally measured temperature and relative humidity (Brutsaert, 2005). The soil heat flux (G) was computed based on soil temperatures (van der Tol, 2012) measured at 2, 5, 15 and 40 cm below the surface (HOBO TMC thermistors) in the YSF. These calculations suggested that G was very small. Similarly, measurement of G with a HFPO1 heat flux plate (Hukseflux, The Netherlands) at 5 cm depth in the SMF suggested G to be <1% of R_n.

2.3. Sap flux density, whole-tree water use and stand water use

2.3.1. Field measurements

The sap flux density (J_p) was measured between 1 October 2014 and 30 September 2015 in twelve trees in the YSF and twenty trees in the SMF using the thermal dissipation probe method (TDP; Granier, 1985). Trees selected for the measurements represented the DBH range and dominant species in the two plots (cf. Reyes-Acosta and Lubczynski, 2014; Table S1). Their DBH ranged from 6 to 22 cm. Each tree was equipped with one TDP-sensor, placed on the southern side of the trunk to minimise sun-exposure and insulated using a locally made radiation shield. Sap flux density (J_p in cm^3 cm^{-2} h^{-1}) was calculated from differences in the temperature using the original empirical equation derived by Granier (1987), and therefore may not represent the correct absolute values of J_p for which species-specific calibrations may be needed (cf. Flo et al. 2019). However, cut-stem segment experiments that are used to derive species-specific calibrations under relatively stable conditions in the laboratory, only provide a snapshot of the performance of a given sap flow method and do not fully portray the natural conditions experienced by plants in the field (Peters et al., 2018; Flo et al., 2019).

The measured natural thermal gradients (NTG) between the two temperature-sensing needles per sensor were <0.2°C for all instrumented trees. Therefore, following Do and Rocheteau (2002), the NTG effect on measured J_p was assumed to be negligible. To account for

circumferential variation in J_p (cf. Alvarado-Barrientos et al., 2013; Nadezhdina et al., 2002), four TDP sensors were inserted at different azimuths (North, South, East and West) in three dominant tree species in the SMF (*A. ditimena, B. ramiflora* and *Cryptocaria*) for at least five continuous days in February and August (Figure S3). The sap flux density values obtained at the four azimuths were used to derive a circumferential correction factor for each period (Ghimire et al., 2014; Lu et al., 2000). The average correction factor (0.99) was used for all trees in the SMF. Circumferential variation in J_P was considered negligible for the small trees in the YSF.

To investigate *radial* variation in J_p, the heat field deformation method (HFD; Nadezhdina et al. (2002) was used. The HFD sensors (ICT international, Australia) consisted of one 1.6 mm diameter heater needle and three temperature-sensing needles.. The HFD probe had eight measurement points (each spaced 10 mm apart), with the first, located 5 mm inwards from the cambium and the last at 75 mm. Radial sap flow patterns were measured in three tree species (*A. ditimena, B. ramiflora* and *Cryptocaria*) in the SMF for at least two consecutive days in October and February. The radial correction factors across the entire sapwood depth were derived following Poyatos et al. (2007) and the average value was applied to all monitored trees in the SMF. Given the small stems of the trees in the YSF (Table 1) and the fact that the ratio of the area of the outermost 2 cm of sapwood (which typically exhibits higher J_p-rates) to the entire sapwood area was greater than 0.78 for all the investigated trees, the effect of radial variation in J_p in the trees of the YSF was considered negligible.

2.3.2. Calculation of stand level transpiration rate (E_t)

Whole-tree water use (sap flow rate Q_t, $cm^3\ h^{-1}$) was estimated by multiplying the sap flux density J_p times the conductive xylem area (A_x, cm^2) for each tree. Sapwood depth was estimated visually from wood cores of 20 trees in the YSF and of 52 trees in the SMF and were verified using a staining method (Grissino-Mayer, 2003; Lubczynski et al., 2017; Rust, 1999). The cores were extracted at the end of the measurement period at breast height using an increment borer.

The water use of the sampled trees was scaled to the stand level to estimate the transpiration per unit area of land (E_t, in mm) for both the YSF and SMF. This was done in three steps. First, simple least-squares regressions between stem cross-sectional stem area (A_s, cm^2) and sapwood area (A_x, cm^2) were derived (YSF: $A_x = 0.94\ A_s - 1.8$, R^2=1.0, n=20; SMF: A_x=0.90 A_s – 7.8, $R^2 = 0.99$, $n = 52$) to estimate stand-level sapwood area from the cross-sectional stem area per plot. We did not observe any heartwood in the majority of the examined trees in the SMF. Therefore, sapwood depth and DBH data for all 52 sampled trees from the SMF were combined to develop a single least-squares regression. The equation was subsequently used with the measured DBH for all trees in the study plots to estimate the total A_x for the SMF. Second, total sap flow per forest site was estimated by multiplying the average sap flux density for all measured trees by the total sapwood area. Note that this neglects any effect of variability in J_p between species because a single overall average value was used for J_p. Several studies have shown that transpiration from a small number of dominant large trees in species-rich tropical montane forest can account for the majority of water lost from a forest canopy (Berry et al., 2017; Horna et al., 2011; McJannet et al., 2007). As such, and in view of the relatively small differences in average sap flux densities between the dominant tree species in the SMF (Table 4), the effect of inter-species variation in J_p on the annual stand-level sap flow total was considered minimal. Finally, to estimate transpiration per unit area of land (E_t), the total daily sap flow was divided by the plot area, corrected for the slope.

2.3.3. Data analysis

Daily average sap flow (Q, $kg\ d^{-1}$) was calculated for the wet season (November–April) and the dry season (May–October) for each measured tree and species. The average Q-values for the dry and the wet season were used in a one-sided paired sample t-test to determine the significance of the difference in average rates for the trees in the YSF and SMF, respectively.

Average sap flow rates at each site were plotted against key micro-meteorological variables and soil water storage. This was done for daily averages, as well as for 30-min averages (excluding values obtained before 07:00 h and after 17:00 h to avoid bias towards extremely low night-time values of Q). Vapour pressure deficits (VPD) were calculated for each site using locally measured humidity and temperature data (cf. Allen et al., 1998). To determine the explanatory power of the meteorological variables and soil water storage for daily average sap flow, the R (Development Core Team, 2011) package "relaimpo" was used with the recommended "lmg" method (Groemping, 2006). The method calculates the relative contribution of each predictor to the R^2 of a linear model but considers the sequence in which the predictors appear in the model. In other words, it partitions the R^2 multiple times by varying the order of the regressors and then takes the average. This analysis was conducted for the entire year, the wet season, and the dry season using the average sap flow data per site. For the SMF, this was also done per sampled tree species.

2.4. Source of transpiration

2.4.1. Field sampling

Stable isotope samples were taken in May 2015 (transition from wet to dry conditions) and August 2015 (cool, dry season). Unfortunately, samples were not collected during the 2015 wet season (January–February). Additional samples were taken in December 2015. December normally marks the start of the wet season but in 2015 the wet season had not started in December and this sampling campaign is instead considered to be representative for the end of the dry season.

During each campaign, xylem samples were taken from seven *Psiadia altissima* trees, three *Lantana camara* shrubs (>1.0 m tall), and three *Rubus* shrubs (>1.0 m, August and December sampling campaigns only) in the YSF. In the SMF, five dominant tree species were sampled: *Abrahamia ditimena, Brachylaena ramiflora, Cryptocaria* sp., *Ocotea samosa* and *Eugenia* spp. (see Table 2 for tree characteristics). Each time, samples were taken from the same set of trees. Samples were obtained by cutting segments from well suberized branches of the trees and shrubs with the help of a ladder (YSF) or by climbing into the tree (SMF).

On the same day as the twig sampling, soil samples were taken at depths of 0–10, 10–20, 30–50, 50–70, 70–90 and 90–110 cm below the surface at two (May 2015) or three (August and December 2015) soil pits (located approximately 10 m from each other) in each plot using a soil auger. All branch and soil samples were immediately stored in 50-ml glass vials and kept refrigerated until analysis.

2.4.2. Laboratory analysis

Water from soil and xylem material was extracted using the cryogenic vacuum distillation method. The extractions and analyses for deuterium (^2H) and oxygen (^{18}O) isotopes were carried out at two

Table 2
Main characteristics (mean ± standard deviation) of the trees and shrubs selected for stable isotope analysis.

Site	Species	Diameter (cm)*	Tree height (m)**
YSF	*Psiadia altissima* (n =7)	8.5 ± 3.5	11.05 ± 8.4
	Lantana camara (n=3)	~2	-
	Rubus moluccanus (n=3)***	~4	-
SMF	*Abrahamia ditimena* (n = 3)	15 ± 0.95	13.3 ± 5.6
	Brachylaena ramiflora (n = 3)	11.3 ± 3.3	10.6 ± 2.7
	Cryptocaria sp. (n = 3)	12.1 ± 4.8	6.6 ± 2.6
	Ocotea samosa (n =3)	7.6 ± 2.0	9.8 ± 2.6
	Eugenia spp. (n = 3)	8.5 ± 3.5	11.05 ± 8.4

* Measured with a diameter tape.
** Determined with a Nikon Forestry Pro Laser Rangefinder.
*** Not sampled in May 2015.

different laboratories. All samples taken in May 2015 (transition from wet to dry season) were sent to the laboratory of the Chair of Hydrology at the University of Freiburg (Germany). Water was extracted using a Koeniger-style system (Koeniger et al., 2011) at ~130°C for 120 min for plant materials and 60 min for soil. The water samples were analysed using a wavelength-scanned cavity ring-down spectrometer (L2130-I, Picarro, USA). Samples suspected to be contaminated with organic carbon compounds were excluded from analysis. The ±1σ measurement uncertainty of the spectrometer was ± 0.16‰ for $\delta^{18}O$ and ± 0.6‰ for $\delta^{2}H$.

All samples collected in September 2015 (dry season) and December 2015 (end of dry season) were sent to the Global Institute for Water Security, University of Saskatchewan, Saskatoon, Canada. The water was extracted from the samples on a Koeniger-style system for 15 min at 200°C. An elementary Isoprime isotope ratio mass spectrometer (IRMS) was coupled with a vaporizing module (A0211 high-precision vaporizer) to eliminate noise from organic compounds (Martín-Gómez et al., 2015). The ±1σ measurement uncertainty was ±0.2‰ and ±1.0‰ for $\delta^{18}O$ and $\delta^{2}H$, respectively.

The isotope ratios are reported using the conventional delta notation relative to the Vienna Standard Mean Ocean Water standard (‰). For all samples, we also calculated the Line Conditioned-Excess (LC-Excess), which is the deviation of $\delta^{2}H$ from the Local Meteoric Water Line (LMWL) (Landwehr and Coplen, 2004). The LMWL was based on 30 precipitation samples from the study sites and a nearby station (< 5 km away at 940 m a.s.l.). Although actual LC-Excess values are affected by the uncertainties in the LMWL, comparisons of LC-excess values are still possible because all samples were compared to the same LMWL.

2.4.3. Isotope-based mixing analysis

The graphical xylem-soil water isotopic comparison (Brunel et al., 1995) and MixSIAR model (Stock et al., 2018; Stock & Semmens, 2016) were used to infer the main source (depth) of water uptake for the three sampling periods. The advantage of the MixSIAR Bayesian framework is that it accounts for uncertainties in the isotopic composition of the soil water and xylem water. The Bayesian mixing model determines the probability distributions of the multiple source contributions. Both site (i.e. YSF or SMF) and tree species were used as fixed effects in the model. Soil samples were pooled as follows: shallow soil (0–10 cm and 10–20 cm; layer D1), which reflects the zone of high saturated hydraulic conductivity (Table 1) and dense rooting (Andriamananjara et al., 2016), the intermediate soil depth (30–50 cm and 50–70 cm; D2), where few roots were observed, and the deep soil (70–90 cm and 90–110 cm; D3), where roots were virtually absent and soil moisture changed very little during the study period (see Results Section 4.1). We did not use an informative prior distribution for the mixing model and set the isotope discrimination factors to zero (i.e., we assumed that fractionation during root water uptake and evaporation from suberized stems was negligible; Ehleringer and Dawson, 1992).

We report both the Bayesian credibility intervals and median values. However, the reported values only provide an approximate indication of the water uptake depth because the isotope-based method has several limitations (see Phillips and Gregg, 2003; Asbjornsen et al., 2007; Penna et al., 2018; Rothfuss and Javaux 2017; Barbeta et al., 2020; von Freyberg et al., 2020). For example, the isotopic composition of soil water tends to vary spatially due to preferential flow, as well as with depth (Sprenger and Allen, 2020) and may depend on the pore sizes sampled (e.g., Sprenger et al., 2019). Furthermore, the method does not take into account the possibility that xylem water can include water from deeper (unsampled) depths in the soil. Cryogenic extraction of soil water, which contains both the mobile water and matrix water (Orlowski et al., 2016; Penna et al., 2018; Beyer and Penna, 2021), may affect the isotopic composition of the soil water. This is particularly an issue for clay-rich soils (Adams et al., 2020; Orlowski and Breuer, 2020; Orlowski et al., 2016; Orlowski et al., 2018). Similarly, a cryogenically extracted water from the trees contains all water from plant tissue, not just the xylem water, and the presence of bark may affect the isotopic composition of the samples (e.g., Zuecco et al., 2020; Nehemy et al., 2022; Barbeta et al., 2022; Engel et al., 2022).Finally, it can take several hours to weeks for water taken up by the roots to reach the canopy (Gaines et al., 2016; Mennekes et al., 2021; Aguzzoni et al. 2022).

2.5. Estimation of total evapotranspiration (ET)

To derive estimates for the seasonal and annual evapotranspiration (ET) for the two sites, the total tree transpiration (E_t) was adjusted to include understorey transpiration. For the more open YSF, understorey transpiration was assumed to be 20% of E_t based on the LAI of the understorey shrubs (~28% of the total LAI; Ghimire et al. (2018)) and partial shading (Motzer et al., 2005). For the denser SMF, a value of 5% was adopted following observations by Holwerda et al. (2016) in a lower montane forest of comparable stature and subject to very similar climatic conditions in Eastern Mexico. Forest floor evaporation (E_s) was simulated using the model of Waterloo et al. (1999) in combination with the measured water-holding capacity for the litter layer for the two sites (van Meerveld et al., 2021). Finally, we added the measured values of interception loss (E_i, based on 66 manual throughfall gauges and three recording troughs, plus five (YSF) to ten (SMF) stemflow gauges per forest (see Ghimire et al., 2017 for details)) to obtain the total ET.

3. Results

3.1. Micrometeorological and soil moisture conditions

Between 1 October 2014 and 30 September 2015, a total of 1629 mm of rain was recorded at the YSF site and 1747 mm at the SMF. Approximately 80% of the total precipitation was delivered during the wet season (November 2014–April 2015) (Fig. 1).

The average daily temperature at both sites was ~19°C (~21°C (both sites) in the wet season versus ~17°C (YSF) and ~16°C (SMF) in the dry season.). Average daily short-wave radiation R_s at the grassland site was 181 W m^{-2} (206 W m^{-2} and 164 W m^{-2} for wet and dry season, respectively; Fig. 1b), representing an overall average daily load of 15.64 MJ m^{-2} d^{-1}. The average daily VPD at both sites was 0.30 kPa, with average daily VPD values of ~ 0.35 kPa in the wet season versus 0.20 kPa (both sites) in the dry season (Fig. 1b and S2). Thus, radiation and VPD were both higher during the warmer wet season than in the cooler dry season. This is reflected in the higher potential evapotranspiration (PET) (calculated according to Turc, 1961) for the wet season (656 mm) than the dry season (494 mm).

Soil moisture content in the top soil layer (5 and 15 cm depths) changed markedly during the study period at both sites, but there was comparatively little seasonal change in soil moisture below 40 cm depth (Fig. 1c and e). Moisture content was consistently higher for the more clayey soil of the YSF than at the SMF, and changes in topsoil moisture at the end of the wet season (March 2015) were larger for the YSF than the SMF (Fig. 1c and e; Table 3).

3.2. Tree transpiration

3.2.1. Diurnal variation in sap flux density during wet and dry seasons

At both sites, average J_p increased rapidly in the morning as VPD and R_s increased, and generally reached a maximum around mid-day, and declined again during the afternoon (Figs. 2 and 3). These diurnal variations in J_p were similar for all species studied in the SMF but were slightly more gradual than for the *Psiadia* trees of the YSF. Pertinently, average J_p did not change appreciably after precipitation events during the dry season at either site (e.g. after the 40 mm event on 20 October 2014, Fig. 3), suggesting that soil moisture availability had a limited impact on transpiration, even at the end of the dry season.

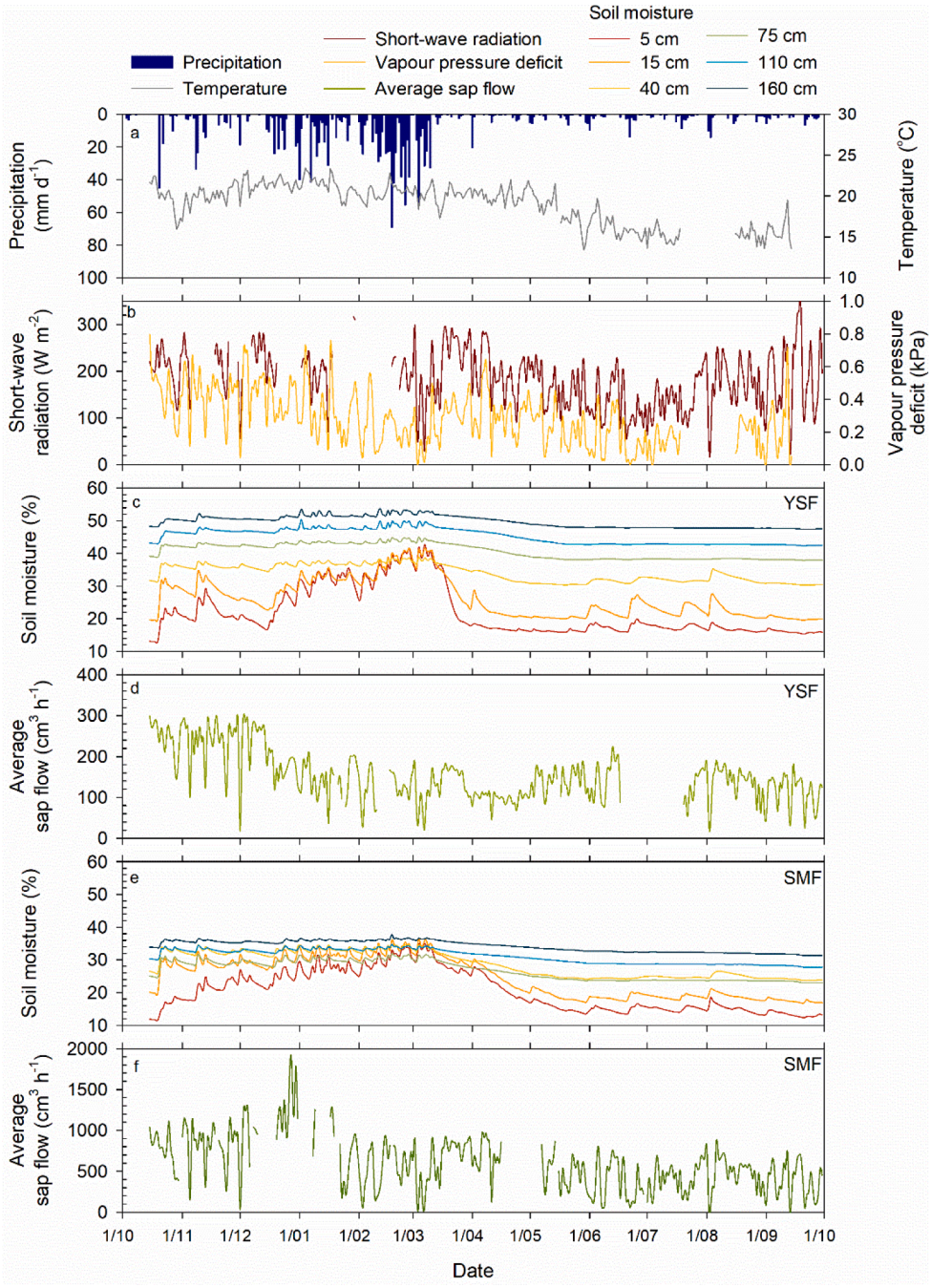

Fig. 1. Time series of (a) daily precipitation (mm d^{-1}) and daily average temperature (°C), (b) vapour pressure deficit (kPa), (c) volumetric soil moisture (%) at different depths, and (d) average day-time sap flow rate (cm^3 h^{-1}) at the YSF, as well as (e) soil moisture and (f) average day-time sap flow at the SMF between 1 October 2014 and 30 September 2015. Panel (b) also shows incoming short-wave radiation (W m^{-2}) measured at a nearby grassland site. Fig. S2 (Supplementary material) gives the corresponding time series for precipitation, temperature and VPD at the SMF. Note the difference in scale for the average daily sap flow rates for the YSF (d) and SMF (f).

Table 3
Average amounts of soil water (mm) stored at different depth intervals in the young secondary forest (YSF) and semi-mature forest (SMF) sites for the wet (November–April) and dry season (May–October). Values in parentheses are the amounts of plant available water (in mm) based on the estimated residual moisture content.

Depth interval	YSF		SMF	
	Wet	Dry	Wet	Dry
0–30 cm	88 (58)	64 (34)	86 (56)	55 (25)
30–70 cm	152 (112)	136 (96)	124 (84)	100 (60)
70–160 cm	425 (335)	390 (300)	294 (204)	260 (170)

3.2.2. *Radial and circumferential variations in sap flux density*

The highest flow rates for three dominant tree species at the SMF (*Abrahamia, Brachylaena* and *Cryptocaria)* were recorded at the outermost (5 mm depth) measurement point (Fig. 4 and Supporting Fig. S3). The rate of decline in J_p with depth differed slightly between species, with maximum values at a depth of 75 mm being 12% of the maximum J_p at the outermost measurement point (*Brachylaena* and *Cryptocaria* sp.) to ~29% (*Abrahamia)* (Fig. 4). Circumferential variations in J_p were very small (Supporting Fig. S4).

3.2.3. *Seasonal variation in sap flow rates*

At both sites, sap flow rates were higher during the warmer, wet season than in the cooler, dry season (Table 4, Fig. 1d and f), but the paired t-test for average seasonal values per tree showed that the differences were statistically significant only for the SMF ($p = 0.001$; versus

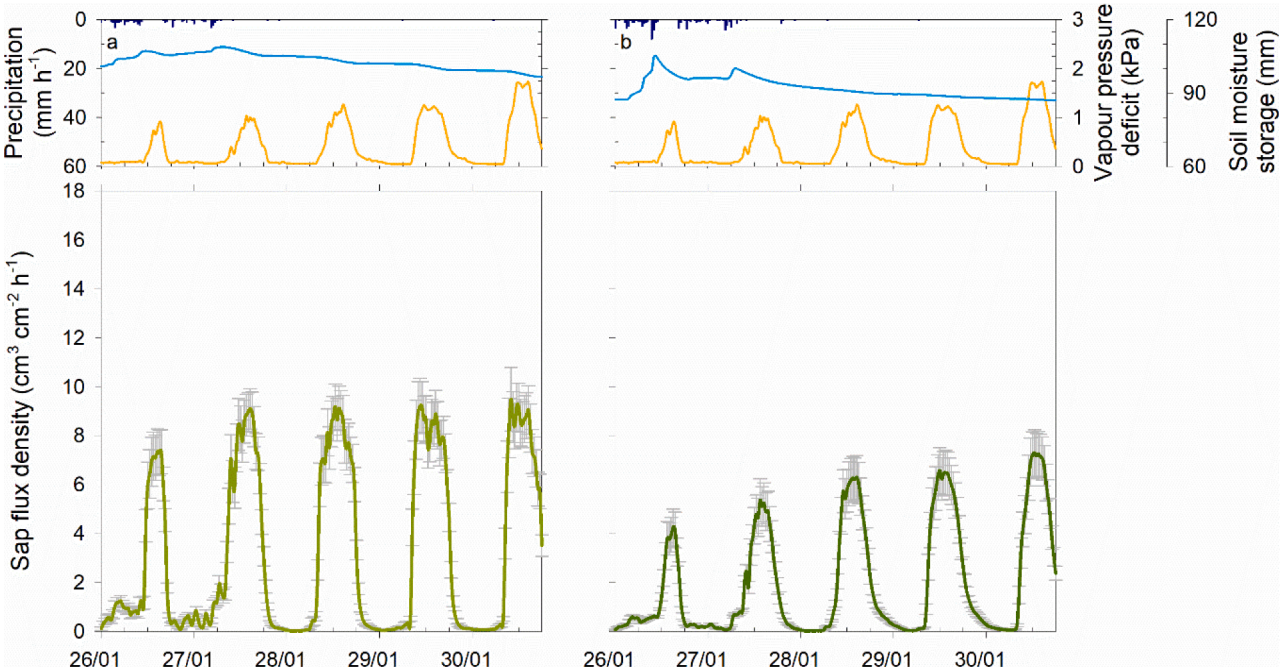

Fig. 2. Diurnal variations in vapour pressure deficit (orange line, top panels) and average sap flux density (J_p) (green lines, bottom panels), along with 30-min precipitation and water storage in the top 30 cm of the soil profile (blue line, top panels) for five days during the warm wet season for (a) the YSF and (b) the SMF study sites. The grey error bars for sap flux density indicate the standard error. (For interpretation of the references to color in this figure legend, the reader is referred to the web version of this article).

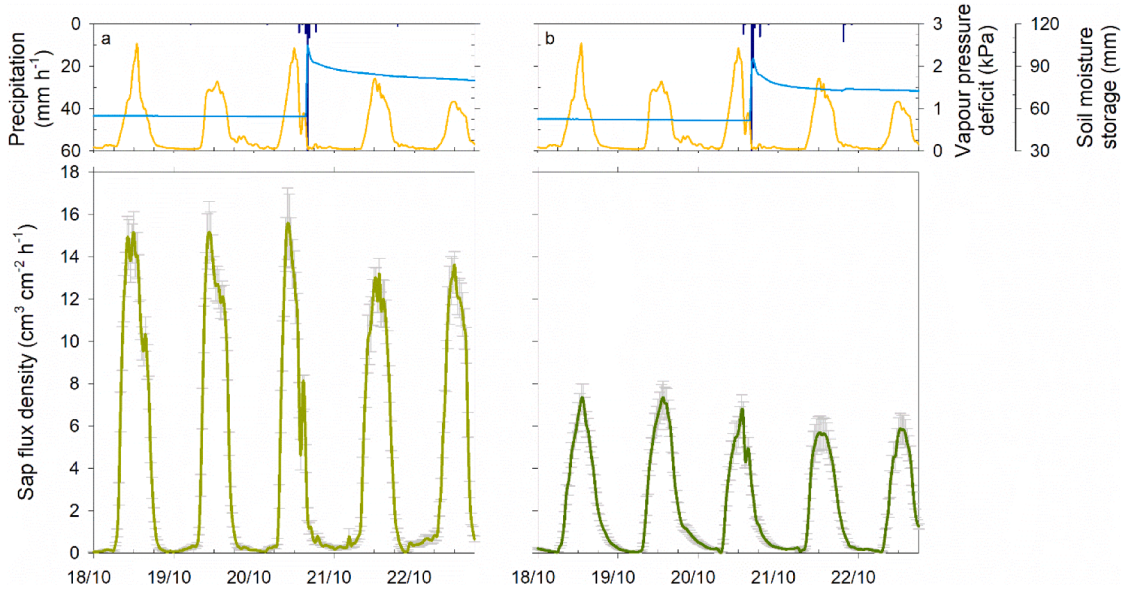

Fig. 3. Diurnal variations in vapour pressure deficit (orange line, top panels) and average sap flux density (J_p) (green lines, bottom panels), along with 30-min precipitation and moisture storage in the top 30 cm of the soil profile (blue line, top panels) for five days during the cool dry season for (a) the YSF and (b) SMF study sites. The grey error bars for sap flux density indicate the standard error. (For interpretation of the references to color in this figure legend, the reader is referred to the web version of this article).

0.251 for the YSF). The ratio of the average wet season sap flow rate to the average dry season sap flow rate varied between a low 1.1 for *Cassipourea* and 3.2 for *Ludia mauritiana*. Whole-tree sap flow rates were highest for *Abrahamia* (15.66 kg d^{-1} in the wet season and 10.69 kg d^{-1} in the dry season) and lowest for *Filicium decipiens* (wet season: 3.97 kg d^{-1}; dry season: 1.72 kg d^{-1}; Table 4). For the *Psiadia* trees of the YSF, sap flow rates differed little between the wet (2.10 kg d^{-1}) and the dry season (1.95 kg d^{-1}), giving a wet season to dry season ratio of 1.1.

3.2.4. *Correlations with climatic factors and soil water storage*

Daily average and 30-min sap flow totals (Q, measured between 7:00 and 17:00 h) increased with VPD up to ~1 kPa, and tended to level off at higher VPD values (Fig. 5a and e). Similarly, increases in R_s resulted in an almost linear increase in sap flow rates up to ~700 W m^{-2}, with smaller increases or no further change in sap flow for higher values of R_s (Fig. 5b and f). Air temperature had to exceed an apparent 'threshold' of ca. ~15°C before sap flow rates increased almost linearly with temperature (Fig. 5c and g). Sap flow was not clearly related to average soil

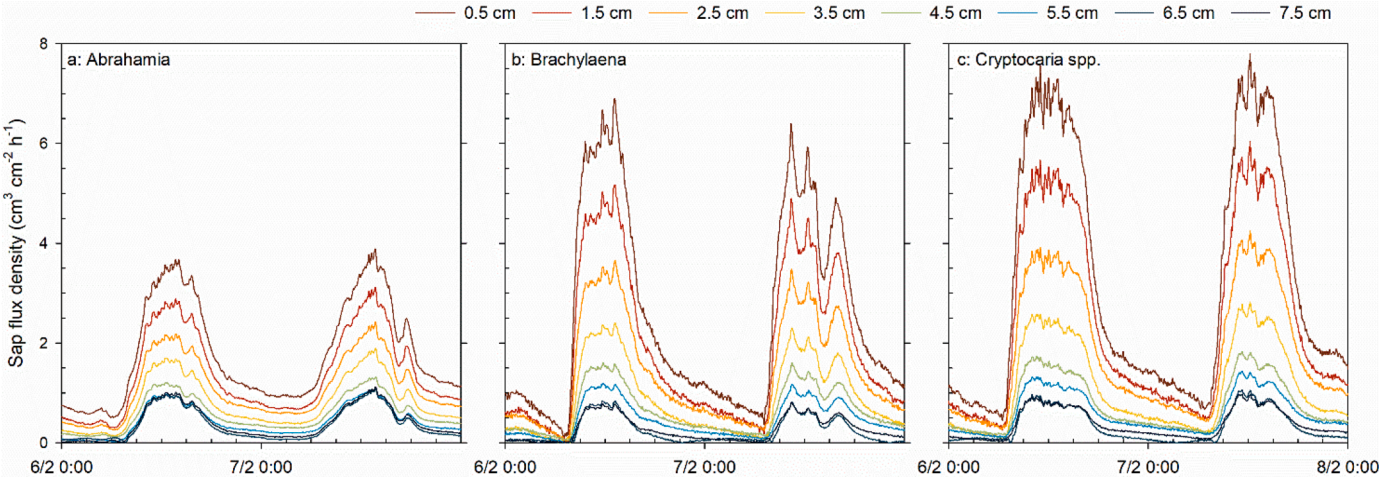

Fig. 4. Radial variation in sap flux density (J_p) for three dominant tree species in the SMF as measured on two days during the wet season. See Fig. S3 for an example of the radial variation in sap flux density during the dry season and Fig. S4 for an example of the circumferential variation in sap flux density.

Table 4
Average daily sap flow rates and sap flux densities for the outer 2 cm of sapwood for the investigated trees in the YSF and SMF in the warm, wet season (November 2014 to April 2015) and the cooler, dry season (May to September 2015 plus October 2014). No standard deviations are given due to the small sample sizes.

Site	Species	Average sap flux density ($cm^3\ cm^{-2}\ h^{-1}$)		Average sap flow rate ($kg\ d^{-1}$)	
		Wet season	Dry season	Wet season	Dry season
YSF	*Psiadia altissima (n = 12)*	3.00	2.94	2.10	1.95
SMF					
	Abrahamia ditimena (n = 5)	2.13	1.54	15.70	10.69
	Brachylaena ramiflora (n = 2)	2.16	1.54	10.10	7.32
	Cryptocaria sp. (n = 3)	1.92	1.68	5.22	4.61
	Ocotea samosa (n = 1)	1.85	1.49	5.48	4.38
	Eugenia spp. (n = 2)	1.24	1.06	5.88	4.96
	Cassipourea (n = 2)	1.74	1.70	4.71	4.45
	Filicium decipiens (n = 1)	1.71	0.75	3.97	1.72
	Erythroxylum spp. *(n = 2)*	1.47	1.23	9.85	8.10
	Ludia mauritiana (n = 1)	1.86	0.60	9.04	2.84
	Leptolaena (n = 1)	0.87	0.80	4.08	3.68

water storage in the top 30 cm of soil (Fig. 5d and h), or any other depth.

The variations in average sap flow for the YSF and SMF, as well as those of the individual species in the SMF, were explained reasonably well by the climatic variables, with VPD and R_s explaining most of the variance (Fig. 6). Only a small part of the variance in sap flow was explained by soil water storage (all three depths together: 18% for the YSF and 10% for the SMF; Fig. 6), but this varied with species and was highest for *Erythroxylum* spp., followed by *Abrahamia* and *Eugenia* spp. (Fig. 6). Surprisingly, the variance in daily sap flow explained by soil water storage was larger for the wet season than for the dry season (Supporting Fig. S5).

3.2.5. Transpiration by the tree stratum and stand evapotranspiration

The total transpiration (E_t) for the tree stratum was 265 mm for the YSF and 462 mm for the SMF. However, the two values were much more comparable after normalising for canopy LAI: 145 mm (YSF) and 136 mm (SMF). For the YSF, E_t was similar for the wet (135 mm; 51% of annual E_t) and the dry season (130 mm; 49%). For the SMF, the wet-season E_t was higher (269 mm; 58% of annual E_t) than the dry-season total (193 mm; 42%).

Total ET amounted to 679 mm y^{-1} (42% of precipitation) for the YSF and 1063 mm y^{-1} (61% of precipitation) for the SMF (Table 5). Overall transpiration (canopy plus estimated understorey transpiration) made up 46–47% of total ET in both forests, while interception evaporation (canopy plus forest floor) contributed 53–54%. Interception was more important than transpiration in the wet season for both sites (58–61% of ET; Table 5).

3.3. Depth of soil water uptake

3.3.1. Isotopic signatures of soil water and xylem water

The xylem and soil water samples taken in May tended to plot below the poorly constrained Local Meteoric Water Line (LMWL) (Fig. 7a-b). In August and December, the soil water samples tended to plot slightly below the LMWL and the xylem water samples slightly above it. However, the majority of the xylem and soil water samples taken in August and December plotted within the 95% prediction band of the precipitation samples (Fig. 7c-f). The average (± SD) Line Conditioned-Excess was –5.8 (±9.0)‰ for all xylem samples from the Psiadia trees of the YSF and -1.17 (±8.5)‰ for all sampled trees in the SMF. Corresponding values for soil water samples from the YSF and SMF were -10.4 (±5.6)‰ and -11.1 (±3.7)‰, respectively.

The soil water isotopic composition tended to be least depleted near the soil surface (layer D1, 0–20 cm depth), except in May (end of wet season) when it was rather similar to that of the deep soil (layer D3, 70-110 cm below the surface; Fig. 8 and Supporting Fig. S6). The variation between soil water samples taken at the same depths and time from different locations within each study plot (i.e., the spatial variation) was largest at the end of the wet season (May) and smallest in the middle of the dry season (August): average standard deviations of soil water $\delta^{18}O$ in May were 0.4‰ (YSF) and 0.8‰ (SMF) versus 0.2‰ (YSF) and 0.3% (SMF) in August (Fig. 8). Differences in isotopic composition of xylem water were smaller at the end of the wet season (average standard deviation for $\delta^{18}O$ of 0.5‰ for the *Psiadia* trees in the YSF and 1.1‰ for the trees in the SMF for the May sampling campaign) than at the end of the dry season (average standard deviation for $\delta^{18}O$ of 0.5 ‰ for the YSF and 1.4 ‰ for the SMF in December 2015) (Figs. 7 and 8). The isotopic composition of xylem water was not related to tree size, except for a weak negative correlation (r_s = -0.57) for the trees in the SMF in December 2015 (Supporting Fig. S7).

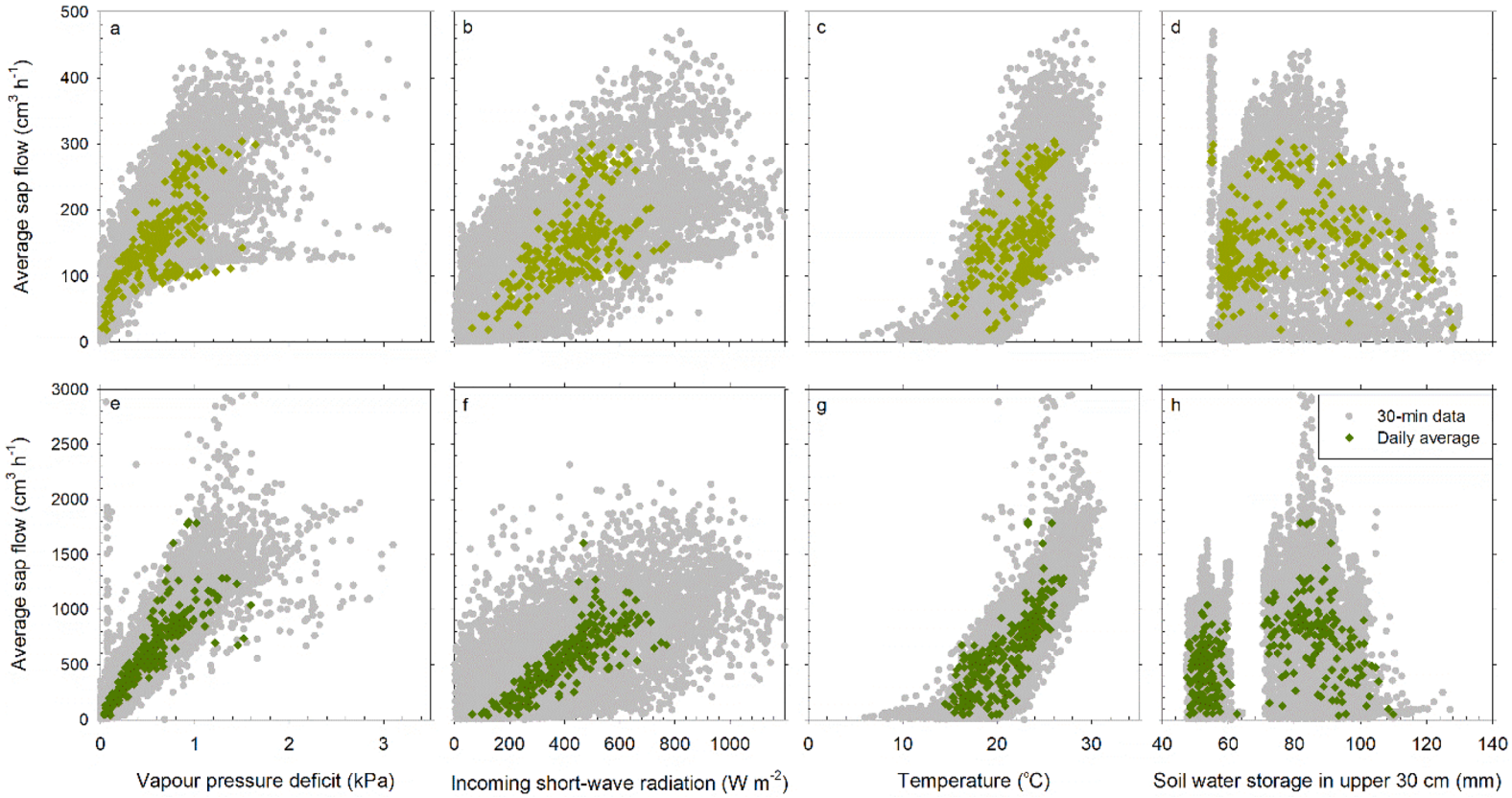

Fig. 5. Average sap flow *Q* between 7:00 and 17:00 (30-min data in grey and daily average values in green) as a function of vapour pressure deficit (panels a, e), incoming short-wave radiation (b, f), air temperature (c, g) and amount of water stored in the upper 30 cm of the soil (d, h) for the YSF (upper row; panels a–d) and the SMF (lower row; e–h). Sap fluxes for individual tree species were highly correlated with the averaged *Q* for all trees (Supporting Table S2). (For interpretation of the references to colour in this figure legend, the reader is referred to the web version of this article).

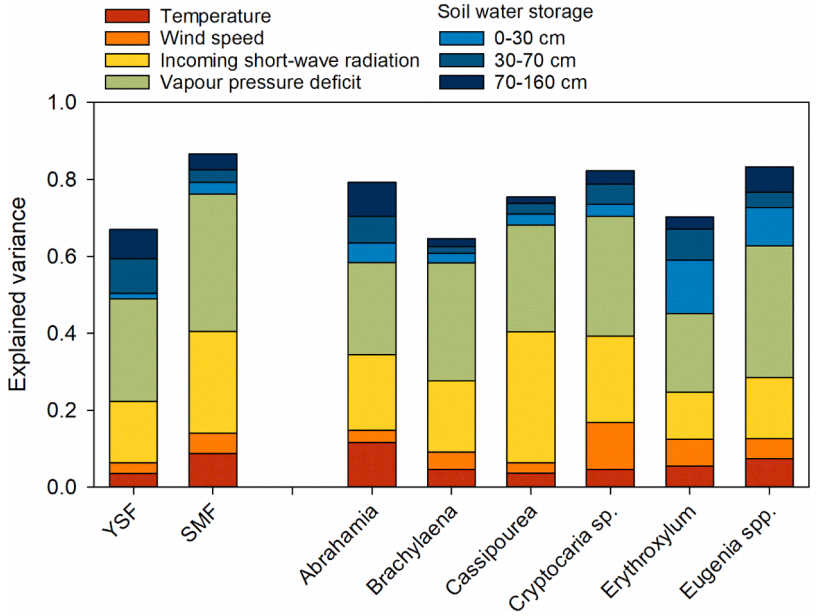

Fig. 6. Proportion of the total variance of average daily sap flow (Q) explained by the four climatic variables and amount of soil water stored in three different depth intervals at the YSF and SMF, and for six dominant tree species in the SMF. For separate results for the wet and dry season, see Supporting Fig. S5.

Table 5
Total precipitation and estimated evapotranspiration (ET) and its components (in mm) for the young secondary forest (YSF) and semi-mature forest (SMF) for the wet (November–April) and dry season (May–October), and the entire study period (October 2014–September 2015). ET components are given in percent of total ET (in parentheses). Total ET was 42% of precipitation for the YSF and 61% of precipitation for the SMF.

	YSF			SMF		
	Wet season	Dry season	Total	Wet season	Dry season	Total
Precipitation (P)	1327	302	1629	1379	368	1747
Total Evapotranspiration (ET)	413	266	679	674	389	1063
Transpiration (E_t)	135	130	265 (39%)	269	193	462 (44%)
Interception loss (E_i)	217	75	292 (43%)	339	140	479 (45%)
Understory transpiration (E_{us})	27	26	53 (8%)	14	10	24 (2%)
Litter evaporation (E_s)	34	35	69 (10 %)	52	46	98 (9%)

3.3.2. Isotope-based mixing analysis

The relatively large variation in the isotopic composition of the soil water between the two pits used for sampling in May and the similarity in the composition of the shallow and deep soil water (Fig. 8a–b) made the mixing analysis results highly uncertain (see the wide 25–75th percentile credibility intervals interval in Fig. 9a–b). Regardless, the results for the SMF suggest that soil water uptake from the deepest layer (D3) was small.

The uncertainty in the mixing ratios was much smaller for the August and December sampling campaigns (judging by the very narrow 25–75th percentile credibility interval, even though the 5–95th percentile interval was still wide). In August, the trees of both the YSF and the SMF took most of their water from layer D2 (40–60 cm below the surface) (Fig. 9c and d). Average tree water uptake in December did not change compared to August for the YSF but for the SMF it shifted to layer D3 (80–100 cm) (Fig. 9e and f). There were, however, large differences between species for the SMF, with *Ocotea* and *Eugenia* still taking up more water from layer D2 than layer D3 in December (Fig. 10 and Supporting Figs. S8–S9). Interestingly, there was no difference in the main depth of water uptake for the *Psiadia* trees and the invasive shrubs in the YSF during the dry season and almost all water uptake there took place from layer D2 (Supporting Fig. S10).

4. Discussion

4.1. Sap flux densities in young and semi-mature secondary tropical forests

The average daily sap flux density (J_p) for the young *Psiadia* trees of the YSF (~3 $cm^3\ cm^{-2}\ h^{-1}$) were higher than those obtained for the trees in the SMF, where wet-season average sap flux densities varied nearly 2.5-fold between species from about 0.9–1.5 $cm^3\ cm^{-2}\ h^{-1}$ (*Leptolaena, Eugenia and Erythroxylum*) to ca. 1.7–2.2 $cm^3\ cm^{-2}\ h^{-1}$ (*Filicium, Cassipourea, Ocotea, Ludia, Abrahamia* and *Brachylaena*; Table 4). Data for other young secondary tropical forests seems to be lacking, but the values fall in the lower range of J_p reported for similarly aged (six years old) native trees grown in (lowland) plantations in Panama (3.0–8.5 $cm^3\ cm^{-2}\ h^{-1}$; Kunert et al., 2012). Likewise, average daily sap flux densities for various 12-year-old native lowland plantation trees in the Philippines ranged from 4.0 to 8.5 $cm^3\ cm^{-2}\ h^{-1}$ (Dierick & Hölscher, 2009).

The average daily sap flux densities of the dominant species in the SMF are also in the lower range of J_p for trees in the upper canopies of various old-growth lower montane rain forests at comparable elevations elsewhere in the tropics (1.7–4.4 $cm^3\ cm^{-2}\ h^{-1}$; Horna et al., 2011; McJannet et al., 2007; Motzer et al., 2005). In structurally complex mature natural forests, such differences between species partly reflect differences in canopy position (Aparecido et al., 2016; Granier et al., 1996; McJannet et al., 2007; Meinzer et al., 1999; Motzer et al., 2005),

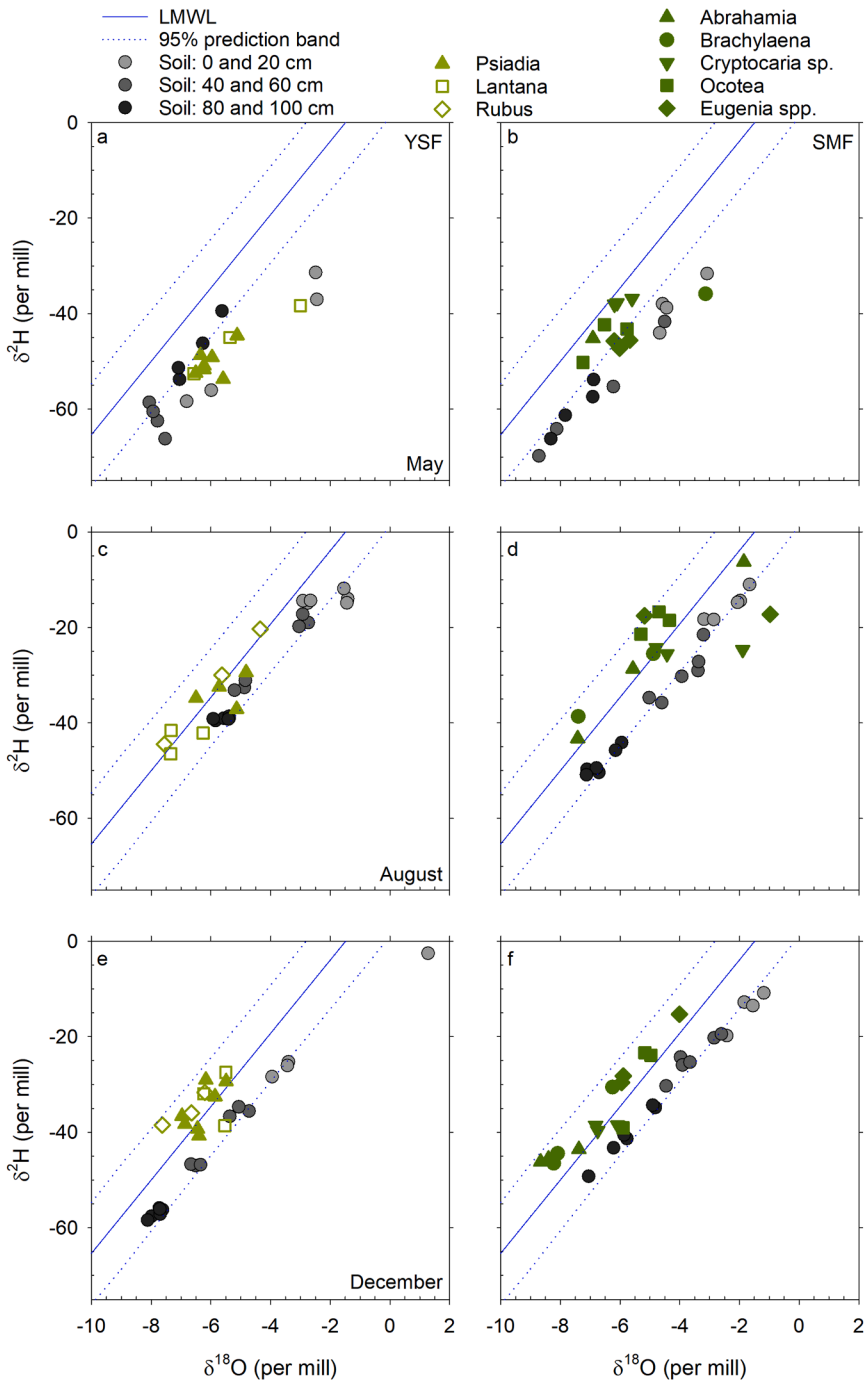

Fig. 7. The δ^2H and $\delta^{18}O$ values for soil water (grey to black symbols) and xylem water samples from the trees (filled light green symbols) and shrubs (open symbols) in the YSF (left-hand panels) and dominant trees (dark green symbols) in the SMF (right-hand panels) at the start of the dry season (May 2015; top row), in mid-dry season (August 2015; central row) and before the start of the wet season (December 2015; bottom row). Different filled green symbols represent different tree species. The blue line represents the LMWL based on 30 precipitation samples ($\delta^2H=7.7\ \delta^{18}O + 11.4$) and the dotted lines the 95% prediction band. (For interpretation of the references to color in this figure legend, the reader is referred to the web version of this article).

as well as rooting depth (Hu et al., 2018; cf. Schwendenmann et al., 2015; Sinacore et al., 2017). However, studies conducted in even-aged, more simply structured mixed tropical tree plantations also reported large variation in sap flux densities between species, suggesting that other factors (e.g., phenology and hydraulic architecture) play a role as well (Dierick and Hölscher, 2009; Kunert et al., 2010, 2012). This is confirmed by the similarly large differences in sap flux densities during the dry season for the different species in the SMF (e.g., *Ocotea* and *Cassipourea* versus *Ludia* and *Filicium*; Table 4) and in some of the mixed tropical tree plantations referred to above (Schwendenmann et al., 2015; Sinacore et al., 2019). Similarly, the comparatively low daily sap flow rates for the trees of the YSF and SMF (2–16 kg d^{-1}; Table 4) are likely to mainly reflect their small size (average DBH < 10 cm; Table 1) compared to old-growth lower montane rain forests at similar elevations elsewhere in the tropics (average DBH typically ~15–17 cm, but with individuals of up to 75–95 cm diameter; Aiba and Kitayama, 1999; Horna et al., 2011; McJannet et al., 2007; Moser et al., 2007).

4.2. *Drivers of transpiration and effect of soil moisture*

Daily average sap flow at both sites showed a strong dependence on VPD and R_s, while soil water availability played a minor role (Figs. 5 and 6). The relative lack of response of sap flow to changes in water content at the study site and many other sites (e.g. Tanaka et al., 2003; Luis et al., 2005; García-Santos et al., 2009) reflects the continued access to soil water (Fig. 1, Table 3, and section 4.3). The ratios of ET/PET (0.59 and 0.92 for the YSF and SMF, respectively) and ET/*P* (0.42 and 0.65, respectively; Table 5) also suggest that ET in the study area is

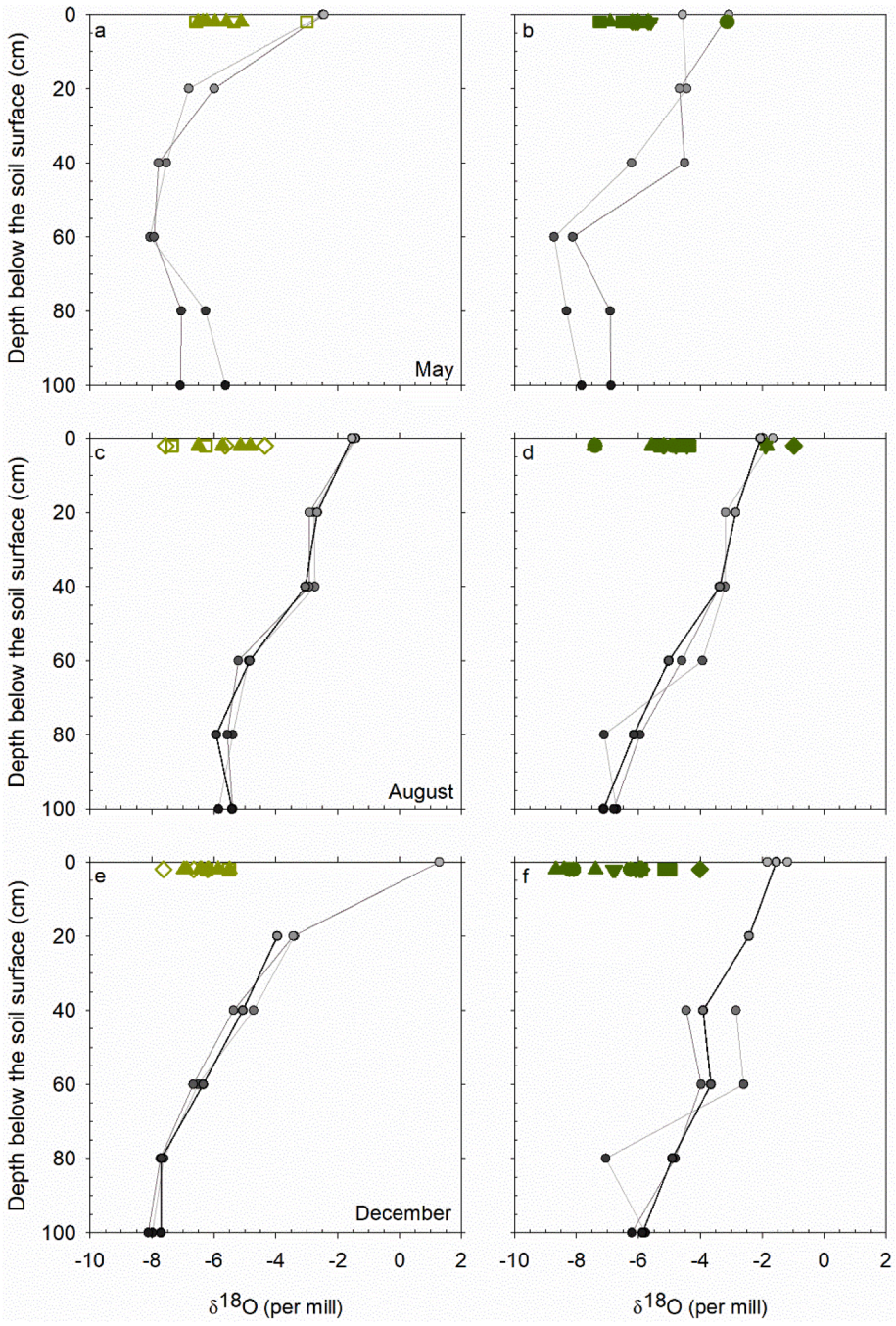

Fig. 8. Depth distributions of $\delta^{18}O$ in soil water (grey to black circles) and xylem water samples (green symbols at top of panels) for *Psiadia* trees in the YSF (left-hand panels) and various trees in the SMF (right-hand panels) at the start of the dry season (May 2015; top row), in mid-dry season (August 2015; central row) and before the start of the wet season (December 2015; bottom row: e-f). Different filled green symbols represent different tree species (see legend of Fig. 7). Results for the invasive shrubs *Lantana* and *Rubus* in the YSF are indicated by open symbols. The values for the soil samples taken from each soil pit are connected by a line. For the corresponding results for $\delta^{2}H$, see Supporting Fig. S6. (For interpretation of the references to color in this figure legend, the reader is referred to the web version of this article).

demand-limited, which fits well with the daily variation in transpiration E_t being explained mostly by variations in VPD and incoming radiation (Figs. 5 and 6).

Relative humidity was very high during parts of the study period and may have reduced transpiration temporarily. High atmospheric humidity in the form of dense fog or wind-driven rain is known to suppress transpiration (Alvarado-Barrientos et al., 2014; García-Santos, 2012) and forest stature (Bruijnzeel et al., 2010). However, because the average interception for the SMF (27% of incident precipitation; Ghimire et al., 2017, Table 5) was effectively equal to the mean rainfall interception (27%) for 15 tropical lower montane rain forests without a significant influence of fog (Bruijnzeel et al., 2011), we assume that fog or wind-driven rainfall were not a very important factor for the low sap flow rates at the study sites.

4.3. Depth of dry-season water uptake

It was not possible to infer the main depth of soil water uptake at the start of the dry season (May 2015) due to the similarity in the isotopic composition of the shallow and deep soil water (Fig. 8a–b). However, based on the rapid decline in soil moisture content in the shallow soil layer (Fig. 1c–e), it is likely that uptake during this time was predominantly from the uppermost 30 cm (cf. Lion et al., 2017; Sohel et al., 2021). For the *Psiadia* trees in the YSF, the main depth of dry-season root water uptake remained between 30 and 70 cm (intermediate soil layer D2), even at the end of the dry season (December 2015; Fig. 10a). The persistently high soil moisture content below 75 cm throughout the dry season (Fig. 1e) also suggests limited water uptake from the subsoil. Thus, although the results of the isotope based mixing analyses are uncertain due to potential issues with the cryogenic extraction of soil

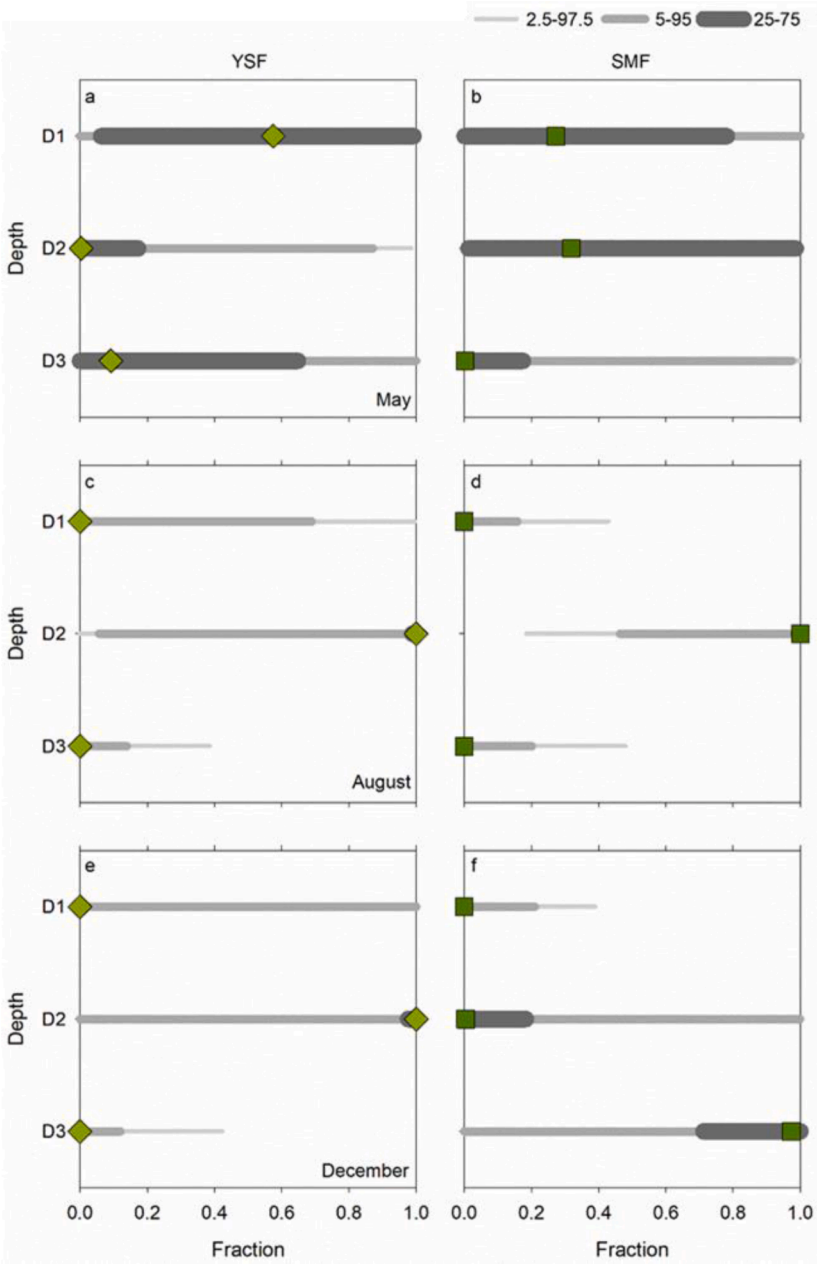

Fig. 9. Median fractions of water uptake from the three depth intervals (green symbols) calculated using the MixSIAR model, and the 2.5–97.5th, 5–95th and 25–75th Bayesian credibility intervals (grey lines) for the May (a, b), August (c, d) and December (e, f) sampling campaigns for the trees in the YSF (left-hand panels a, c, e) and the SMF (right-hand panels b, d, f). (For interpretation of the references to color in this figure legend, the reader is referred to the web version of this article).

and xylem water (Adams et al., 2020; Orlowski and Breuer, 2020; Orlowski et al., 2018) and the isotopic offset between the soil and plant water samples (Fig. 7b–f), the results appear plausible.

Comparative information on the depth of soil water uptake by young tropical secondary vegetation seems to be limited to soil water observations made beneath a ca. four-year-old regrowth in Eastern Amazonia. At that site, with demonstrated fine roots down to at least 6 m, three quarters of wet-season transpiration came from a depth of 0–90 cm (Sommer et al., 2003). For even younger vegetation at the same location, Hölscher et al. (1997) concluded that soil water uptake below 100 cm depth would have been necessary to maintain the high transpiration rates. Re-sprouting of stumps and surviving roots were important for the rapid development of biomass in this case (LAI = 4.2; Sommer et al. (2003)). This is different from the more impoverished soil conditions at the YSF (LAI = 2.3) following repeated slash-and-burn cycles and associated loss of soil fertility (Styger et al., 2007).

There were no major differences in the main depth of uptake between the trees and the invasive shrubs in the YSF as the dry season progressed (Supporting Fig. S10). However, the isotopic composition of the xylem water of the *Lantana* shrubs was more depleted than that of the *Psiadia* trees; the isotopic composition of *Rubus* was more variable in August (Fig. 7c). Transpiration rates for *Psiadia* did not change notably during the dry season (Table 4; cf. Ghimire et al. (2018)), but measurements of stomatal conductance for the shrubs indicated that soil moisture was a limiting factor, suggesting the shrubs were more sensitive to moisture deficits than the trees (Ghimire et al., 2018).

In the SMF, the trees mainly took water from intermediate depths (layer D2; 30–50 and 50–70 cm samples) in the middle of the dry season (August), but by the end of the dry season (December), a shift to deeper layers (D3; 70–90 cm and 90–110 cm samples) was inferred for some

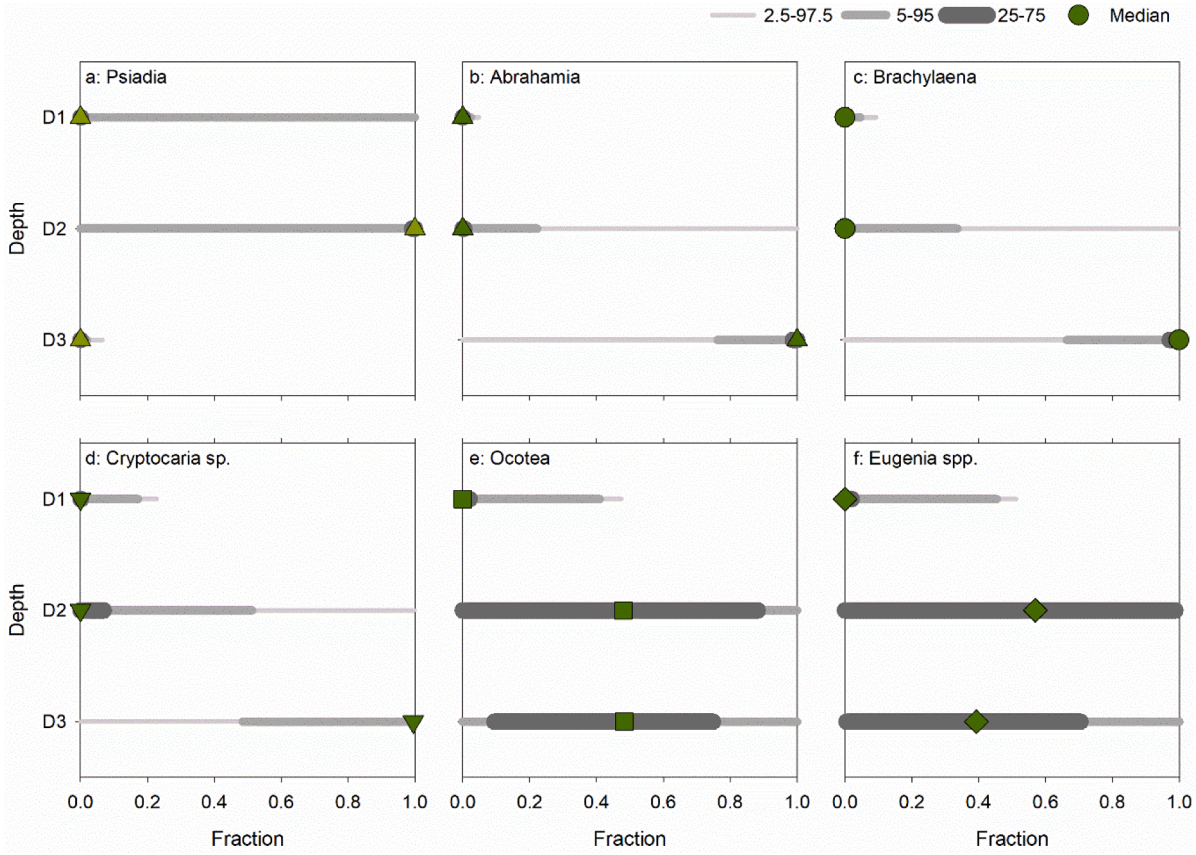

Fig. 10. Median fractions of soil water uptake from the three depth intervals (D1–D3) in December 2015 calculated using the MixSIAR model (green symbols) and their 2.5–97.5th, 5–95th and 25–75th Bayesian credibility intervals (grey lines) for *Psiadia* trees in the YSF (a) and the dominant tree species in the SMF (b–f). For the corresponding results for May and August 2015, see Supporting Fig.s S8 and S9, respectively. (For interpretation of the references to color in this figure legend, the reader is referred to the web version of this article).

species (*Abrahamia* and *Brachylaena;* Fig. 10 and Supporting Figures S8–9). Studies in species-rich lowland rain forests have shown that (smaller) evergreen trees and shrubs tend to rely more on deeper soil water as the dry season progresses and are largely able to maintain high transpiration rates, whereas (mostly larger) deciduous trees use shallower soil water (e.g., Meinzer et al., 1999; Stahl et al., 2013). In a lowland rain forest in Malaysia, uptake was mostly from the top 50 cm during wet periods but shifted to deeper depths during dry periods (Lion et al., 2017). Only during occasional very dry periods did trees access deeper and more tightly bound older water (Lion et al., 2017). A different pattern has been described by Muñoz-Villers et al. (2018) for a marginal cloud forest site in Mexico, where upper canopy trees increasingly used shallow (0–30 cm) soil water and transpiration rates declined towards the end of the dry season. This shift was attributed to a lack of nutrients in the subsoil. The general lack of fertility of the heavily leached soils (Bailly et al., 1974), may have reduced transpiration at the study sites as well (as also reflected by the low LAI), but there was sufficient water available for transpiration, even at the end of the dry season (Fig. 1e).

Temporal changes in the main depth of root water uptake by the trees in the SMF were species-dependent (Fig. 10 and Supporting Figs. S8–9). The change in the depth of water uptake between the middle and the end of the dry season was most pronounced for *Abrahamia* and *Brachylaena* (Fig. 10 and Supporting Figs. S8–9), two species for which the differences in average sap flux densities between the wet and the dry season were large (Table 4). Thus, even though *Abrahamia* and *Brachylaena* may have shifted their uptake towards deeper water sources, this did not allow them to maintain an equally high water uptake rate. This is contrary to some other studies showing that species that used deeper water sources were able to maintain high transpiration rates during drier periods (e.g., Jackson et al., 1995). Indeed, a shift to deeper soil water uptake towards the end of the dry season was also observed for *Cryptocaria* (Figs. 10 and S8–9), for which the average transpiration rate differed little between the wet and dry season (Table 4). Differences in average wet- and dry-season transpiration rates were also relatively small for *Ocotea* and *Eugenia*, but for these species, the main depth of water uptake did not appear to change over time (Fig. 10 and Supporting Fig. S9).

Several studies have shown a relation between the isotopic composition of xylem water (and thus depth of water uptake) and the size of the trees (e.g., Hardanto et al., 2017; Schwendenmann et al., 2015). In a species-rich upland rain forest in northern Queensland with a similar rainfall regime (1680 mm y^{-1}), the majority of the 46 examined tree species relied primarily on water in the top 20 cm of the soil, although larger and faster-growing trees preferentially took up water below 20 cm depth (Sohel et al., 2021). We did not find such a relation (Supporting Fig. S7). This is likely because of by the limited range in sampled tree sizes, but may also indicate that the different trees took water from similar depths (Lion et al., 2017). Only at the end of the dry season (December) did a weak negative correlation between tree DBH and the isotopic composition of xylem water become apparent (Supporting Fig. S7f). By then, soil water had become more depleted at greater depth (Fig. 8f). The isotopically more depleted xylem water in December may therefore indicate that the larger trees had access to deeper soil water (cf. Bretfeld et al., 2018).

4.4. Total evapotranspiration

Total ET during the 1 October 2014 to 30 September 2015 study period was estimated to be 679 mm y^{-1} for the YSF, of which ~47% occurred via transpiration (trees plus understorey) and 53% via wet-canopy and forest floor evaporation (Table 5). This is 11% lower than the water budget-based ET derived for a nearby catchment with mature montane rainforest (1195 mm y^{-1}) for years with comparable rainfall as our study period (Bailly et al., 1974). For the SMF, the total ET was estimated at 1063 mm, of which 46% occurred via transpiration and 54% via interception losses (Table 5). Although values for understorey and forest floor evaporation were not measured but estimated using (empirical) models, the derived estimates for total ET are plausible in light of the elevation (950–990 m a.s.l.) and comparatively low LAI of the study sites compared to most other secondary tropical forest sites for which annual evapotranspiration values are available (Supporting Table S3).

Comparing the combined total of transpiration and forest floor evaporation ($E_t + E_s$) for young to intermediate secondary tropical forests and normalising for net radiation input (R_n), gives values of 0.22 and 0.34 for the YSF and SMF, respectively. These are much lower than the values reported for 3–20 year-old regenerating forests in different parts of lowland Amazonia (0.62–0.67; $n = 4$) or a 20-year-old montane forest in Eastern Mexico (0.59; Fig. 11 and Supporting Table S3). A comparably low E_t/R_n ratio of ca. 0.36 was inferred only for eight-year-old regrowth in Panamá during an exceptional drought (Bretfeld et al., 2015; Supporting Table S3 and Fig. 11). The reason for this striking contrast in relative transpiration rates between the two Malagasy study sites and Amazonian regrowth likely reflects the combination of the much more vigorous growth and canopy development at the Amazonian sites (LAI 4.2–5.7) due to re-sprouting of stumps and a deep surviving root network (Sommer et al., 2003), plus advected energy from adjacent warmer, deforested sites (Giambelluca et al., 2000; Hölscher et al., 1997; cf. Kunert et al., 2015). In contrast, the lower temperatures at the study sites, combined with the degraded soil conditions after repeated slash-and-burn cycles at the YSF (Bailly et al., 1974; Styger et al., 2007) and poor subsoil drainage (both YSF and SMF; Zwartendijk et al. (2020)), may have resulted in slow growth and a low LAI (Fig. 11b). Indeed, plotting reported values of $(E_t + E_s)/R_n$ against forest LAI suggests an increase in the ratio until an LAI of 4–5 after which $(E_t + E_s)/R_n$ tends to stabilise or possibly declines somewhat (Fig. 11b). Nevertheless, after also normalising $(E_s + E_t)/R_n$-values for the respective forests by their LAI, the values for both the YSF and SMF (0.10–0.12) turn out to be effectively the same as those derived for ca. 20-year-old regenerating stands in lowland Amazonia (site ZF3) and montane Eastern Mexico (Veracruz site, Supporting Fig. S11b and Supporting Table S3). Moreover, ratios for young to intermediate secondary forests normalised this way do not seem to differ from those for old-growth forests, with the exception of several Amazonian and South-east Asian sites where transpiration rates were considered to be strongly affected by advection of sensible heat from warmer, deforested neighbouring areas (Giambelluca et al., 2000; Hölscher et al., 1997; Sommer et al., 2003; Fig. 11b and Table S3). However, the database is extremely small, particularly for montane forests (Supporting Table S3) and more work is needed to confirm or refute these contentions. Furthermore, comparisons of forest transpiration between (distant) sites requires caution because of differences in climatic conditions (radiation load, precipitation seasonality), forest type and age, and hence species composition, density and structure, as well as the size of the trees (McJannet et al., 2007; Von Randow et al., 2019). A direct comparison of transpiration totals from the monodominant YSF with other, more species-rich forests requires further caution.

5. Conclusions

Transpiration was examined in a young (5–7 years) and a semi-mature (most trees ~20 years old) forest in montane eastern Madagascar. Vapour pressure deficit and net radiation were the main drivers of the variations in daily transpiration; soil moisture availability played a minor role. Trees in the younger forest relied mainly on moisture from the intermediate soil depth (30–70 cm). For three out of five dominant canopy species in the SMF (*Abrahamia ditimena, Brachylaena ramiflora* and *Cryptocaria* sp.) there was a change in the depth of water uptake at the end of the dry season, indicating some evidence of complementary resource use. A comparison of evaporative losses (normalised by net radiant energy inputs) from the study sites with secondary and selected old-growth forests across the tropics suggests that the transpiration rates and LAI values for the study sites are low. This is thought to mainly reflect the poor soil fertility rather than seasonal water stress or climatic limitations to vegetation growth. Moreover, the observed relatively high difference in evapotranspiration totals between the young forest (679 mm y^{-1}) and the semi-mature forest (1063 mm y^{-1}) underscores the need to take the stage of forest regrowth into account when assessing the hydrological impacts of land-cover change in the study area.

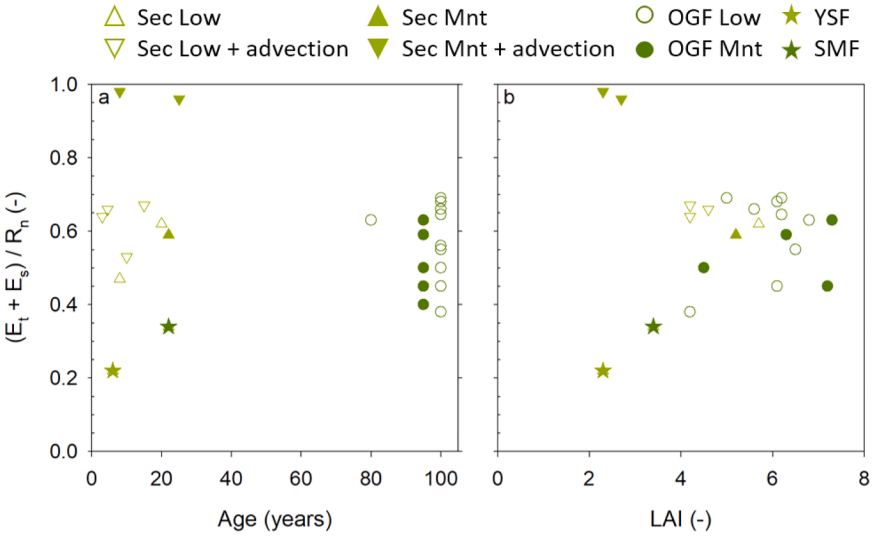

Fig. 11. Apparent transpiration (E_t + forest floor evaporation, E_s) for regenerating tropical forest scaled by net radiation (R_n) as a function of (a) forest age and (b) leaf area index (LAI). Lowland secondary forest sites are indicated by open triangles, and montane secondary forest sites by filled triangles. Sites affected by advection are indicated by downward-pointing triangles. The two stars mark the two study sites of this study (YSF and SMF). Selected old-growth forests (OGF) have been added for comparison and are shown by circles at an age of 100 years (lowland sites) or 95 years (montane sites) to avoid clutter. Data and references are listed in Supporting Table S3. For the relations between forest age and LAI or the apparent transpiration scaled by both net radiation and LAI ([$(E_t + E_s)$ / R_n] / LAI), see Supporting Fig. S11.

CRediT authorship contribution statement

Chandra Prasad Ghimire: Methodology, Investigation, Formal analysis, Writing – original draft, Writing – review & editing. **H.J. (Ilja) van Meerveld:** Supervision, Methodology, Formal analysis, Writing – original draft, Writing – review & editing. **Bob W. Zwartendijk:** Investigation, Formal analysis, Writing – review & editing. **L. Adrian Bruijnzeel:** Validation, Formal analysis, Writing – original draft, Writing – review & editing. **Maafaka Ravelona:** Investigation. **Jaona Lahitiana:** Investigation. **Maciek W. Lubczynski:** Validation, Writing – review & editing.

Declaration of Competing Interest

The authors declare that they have no known competing financial interests or personal relationships that could have appeared to influence the work reported in this paper.

Data Availability

Data will be made available on request.

Acknowledgements

This work was part of the P4GES (Can Paying 4 Global Ecosystem Services values reduce poverty?) project (www.p4ges.org) funded by the Ecosystem Services for Poverty Alleviation programme of the United Kingdom (grant no. NE/K010417/1). We are grateful to Jean Yves Andrianavonona, Georges Ramarolahy, Jean-Claude Randriatahina, Jean Marcel Razafimanantsoa, Rolland Tsiresy, René Fréderic Razafimahepa, Youssouf and Mad Randrianasolo for their indispensable help in the field. We thank the staff of the Mitsinjo Association (https://associationmitsinjo.wordpress.com) for allowing access to the sites, the Laboratoire des Isotopes (University of Antananarivo) for logistical support, Kim Janzen (Institute for Global Water Security, Canada) and Barbara Herbstritt (University of Freiburg, Germany) for isotope analysis, project leader Julia Jones (Bangor University) for support and encouragement, and Murat Ucer (University of Twente) for the supply of equipment. We further thank Tom Giambelluca (University of Hawai'i) for unpublished LAI values for the Pang Khum sites and Steve Paton (Smithsonian Institution, Panama) for net radiation data for the Agua Salud sites. Jun Zhang (EMSA–TNO, The Netherlands) is thanked for her help with Figs. 11 and S11 and Vincent Odongo (International Livestock Research Institute, Kenya) for help with analysing soil heat flux data . Bob W. Zwartendijk acknowledges financial support from the Dutch Research Council (NWO) (Grant no. 023.016.033). The manuscript benefitted from the constructive comments from two anonymous reviewers and the editor.

Supplementary materials

Supplementary material associated with this article can be found, in the online version, at doi:10.1016/j.agrformet.2022.109159.

References

Adams, R.E., Hyodo, A., SantaMaria, T., Wright, C.L., Boutton, T.W., West, J.B., 2020. Bound and mobile soil water isotope ratios are affected by soil texture and mineralogy, whereas extraction method influences their measurement. Hydrol. Processes 34 (4), 991–1003. https://doi.org/10.1002/hyp.13633.

Aguzzoni, A., Engel, M., Zanotelli, D., Penna, D., Comiti, F., Tagliavini, M., 2022. Water uptake dynamics in apple trees assessed by an isotope labeling approach. Agric. Water Manage. 266, 107572 https://doi.org/10.1016/j.agwat.2022.107572.

Aiba, S., Kitayama, K., 1999. Structure, composition and species diversity in an altitude-substrate matrix of rain forest tree communities on Mount Kinabalu, Borneo. Plant Ecol. 140 (2), 139–157. https://doi.org/10.1023/A:1009710618040.

Alkama, R., Cescatti, A., 2016. Biophysical climate impacts of recent changes in global forest cover. Science 351(6273), 600-604. doi:10.1126/science.aac8083.

Allen, R.G., Pereira, L.S., Raes, D., Smith, M., 1998. Crop Evapotranspiration – Guidelines for Computing Cop Water Requirements. FAO, Rome.

Alvarado-Barrientos, M.S., Hernández-Santana, V., Asbjornsen, H., 2013. Variability of the radial profile of sap velocity in Pinus patula from contrasting stands within the seasonal cloud forest zone of Veracruz, Mexico. Agric. For. Meteorol. 168, 108–119. https://doi.org/10.1016/j.agrformet.2012.08.004.

Alvarado-Barrientos, M.S., Holwerda, F., Asbjornsen, H., Dawson, T.E., Bruijnzeel, L.A., 2014. Suppression of transpiration due to cloud immersion in a seasonally dry Mexican weeping pine plantation. Agric. For. Meteorol. 186, 12–25. https://doi.org/10.1016/j.agrformet.2013.11.002.

Amin, A., Zuecco, G., Geris, J., Schwendenmann, L., McDonnell, J.J., Borga, M., Penna, D., 2020. Depth distribution of soil water sourced by plants at the global scale: a new direct inference approach. Ecohydrology 13 (2), e2177. https://doi.org/10.1002/eco.2177.

Andréassian, V., 2004. Waters and forests: from historical controversy to scientific debate. J. Hydrol. 291 (1), 1–27. https://doi.org/10.1016/j.jhydrol.2003.12.015.

Andriamananjara, A., Hewson, J., Razakamanarivo, H., Andrisoa, R.H., Ranaivoson, N., Ramboatiana, N., Razafindrakoto, M., Ramifehiarivo, N., Razafimanantsoa, M.-P., Rabeharisoa, L., Ramananantoandro, T., Rasolohery, A., Rabetokotany, N., Razafimbelo, T., 2016. Land cover impacts on aboveground and soil carbon stocks in Malagasy rainforest. Agric. Ecosyst. Environ. 233, 1–15. https://doi.org/10.1016/j.agee.2016.08.030.

Aparecido, L.M.T., Miller, G.R., Cahill, A.T., Moore, G.W., 2016. Comparison of tree transpiration under wet and dry canopy conditions in a Costa Rican premontane tropical forest. Hydrol. Processes 30 (26), 5000–5011. https://doi.org/10.1002/hyp.10960.

Asbjornsen, H., Mora, G., Helmers, M.J., 2007. Variation in water uptake dynamics among contrasting agricultural and native plant communities in the Midwestern U.S. Agriculture. Ecosyst. Environ. 121 (4), 343–356. https://doi.org/10.1016/j.agee.2006.11.009.

Bailly, C., de Coignac, G.B., Malvos, C., Ninggre, J.M., Sarailh, J.M., 1974. Étude de l'influence du couvert naturel et de ses modifications á Madagascar. Expérimentations en bassins versants élémentaires. Cahiers Scientifiques, 4. Centre Scientifique Forestier Tropical, Nogent-sur-Marne, France, p. 114.

Barbeta, A., Gimeno, T.E., Clavé, L., Fréjaville, B., Jones, S.P., Delvigne, C., Wingate, L., Ogée, J., 2020. An explanation for the isotopic offset between soil and stem water in a temperate tree species. New Phytol. 227, 766–779. https://doi.org/10.1111/nph.16564.

Barbeta, A., Burlett, R., Martín-Gómez, P., Fréjaville, B., Devert, N., Wingate, L., Domec, J.-C., Ogée, J., 2022. Evidence for distinct isotopic compositions of sap and tissue water in tree stems: consequences for plant water source identification. New Phytol. 233, 1121–1132. https://doi.org/10.1111/nph.17857.

Berry, Z.C., Looker, N., Holwerda, F., Gómez Aguilar, L.R., Ortiz Colin, P., González Martínez, T., Asbjornsen, H., 2017. Why size matters: the interactive influences of tree diameter distribution and sap flow parameters on upscaled transpiration. Tree Physiol. 38 (2), 263–275. https://doi.org/10.1093/treephys/tpx124.

Beyer, M., Penna, D., 2021. On the spatial-temporal under-representation of isotopic data in ecohydrological studies. Biomimetic Bioinspired Membr. New Front. Sustain. Water Treat. Technol. 3, 643013 https://doi.org/10.3389/frwa.2021.643013.

Bonan, G.B., 2008. Forests and climate change: forcings, feedbacks, and the climate benefits of forests. Science 320 (5882), 1444–1449. https://doi.org/10.1126/science.1155121.

Bonan, G.B., 2016. Forests, climate, and public policy: a 500-year interdisciplinary odyssey. Annu. Rev. Ecol. Evol. Syst. 47 (1), 97–121. https://doi.org/10.1146/annurev-ecolsys-121415-032359.

Bretfeld, M., Ewers, B.E., Hall, J.S., 2018. Plant water use responses along secondary forest succession during the 2015–2016 El Niño drought in Panama. New Phytol. 219 (3), 885–899. https://doi.org/10.1111/nph.15071.

Bruijnzeel, L.A., Kappelle, M., Mulligan, M., Scatena, F.N., 2010. Tropical montane cloud forests: state of knowledge and sustainability perspectives in a changing world. In: Bruijnzeel, L.A., Scatena, F.N., Hamilton, L.S. (Eds.), Tropical Montane Cloud Forests, Science for Conservation and Management. Cambridge University Press, Cambridge, UK, pp. 691–740.

Bruijnzeel, L.A., Mulligan, M., Scatena, F.N., 2011. Hydrometeorology of tropical montane cloud forests: emerging patterns. Hydrol. Processes 25 (3), 465–498. https://doi.org/10.1002/hyp.7974.

Brunel, J.-P., Walker, G.R., Kennett-Smith, A.K., 1995. Field validation of isotopic procedures for determining sources of water used by plants in a semi-arid environment. J. Hydrol. 167 (1), 351–368. https://doi.org/10.1016/0022-1694(94)02575-V.

Brutsaert, W., 2005. Hydrology: an Introduction. Cambridge University Press, Cambridge, UK, p. 605.

Chazdon, R., 2014. Second Growth: the Promise of Tropical Forest Regeneration in an Age of Deforestation. University of Chicago Press, Chicago, USA.

Curtis, P. G., Slay, C. M., Harris, N. L., Tyukavina, A., Hansen, M. C., 2018. Classifying drivers of global forest loss. Science 361(6407), 1108-1111. doi:10.1126/science.aau3445.

Devaraju, N., Bala, G., Nemani, R., 2015. Modelling the influence of land-use changes on biophysical and biochemical interactions at regional and global scales. Plant Cell Environ. 38 (9), 1931–1946. https://doi.org/10.1111/pce.12488.

Dierick, D., Hölscher, D., 2009. Species-specific tree water use characteristics in reforestation stands in the Philippines. Agric. For. Meteorol. 149 (8), 1317–1326. https://doi.org/10.1016/j.agrformet.2009.03.003.

Do, F., Rocheteau, A., 2002. Influence of natural temperature gradients on measurements of xylem sap flow with thermal dissipation probes. 2. Advantages and calibration of a noncontinuous heating system. Tree Physiol. 22 (9), 649–654. https://doi.org/10.1093/treephys/22.9.649.

Ehleringer, J.R., Dawson, T.E., 1992. Water uptake by plants: perspectives from stable isotope composition. Plant Cell Environ. 15 (9), 1073–1082. https://doi.org/10.1111/j.1365-3040.1992.tb01657.x.

Ellison, D., Morris, C.E., Locatelli, B., Sheil, D., Cohen, J., Murdiyarso, D., Gutierrez, V., Noordwijk, M.v., Creed, I.F., Pokorny, J., Gaveau, D., Spracklen, D.V., Tobella, A.B., Ilstedt, U., Teuling, A.J., Gebrehiwot, S.G., Sands, D.C., Muys, B., Verbist, B., Sullivan, C.A., 2017. Trees, forests and water: cool insights for a hot world. Glob. Environ. Chang. 43, 51–61. https://doi.org/10.1016/j.gloenvcha.2017.01.002.

Engel, M., Frentress, J., Penna, D., Andreoli, A., van Meerveld, I., Zerbe, S., Tagliavini, M., Comiti, F., 2022. How do geomorphic characteristics affect source of tree water uptake in restored river floodplains. Echohydrology. https://doi.org/10.1002/eco.2443.

FAO, 2016. Global Forest Resources Assessment 2015. How are the World's Forests Changing? FAO, Rome, Italy.

Flo, V., Martinez-Vilalta, Steppe, K., Schuldt, B., Poyatos, R., 2019. A synthesis of bias and uncertainty in sap flow methods. Agric. For. Meteorol. 271, 362–374. https://doi.org/10.1016/j.agrformet.2019.03.012.

Foley, J.A., Asner, G.P., Costa, M.H., Coe, M.T., DeFries, R., Gibbs, H.K., Howard, E.A., Olson, S., Patz, J., Ramankutty, N., Snyder, P., 2007. Amazonia revealed: forest degradation and loss of ecosystem goods and services in the Amazon Basin. Front. Ecol. Environ. 5 (1), 25–32. https://doi.org/10.1890/1540-9295(2007)5[25:ARFDAL]2.0.CO;2.

Gaines, K.P., Meinzer, F.C., Duffy, C.J., Thomas, E.M., Eissenstat, D.M., 2016. Rapid tree water transport and residence times in a Pennsylvania catchment. Ecohydrology 9, 1554–1565. https://doi.org/10.1002/eco.1747.

García-Santos, G., 2012. Transpiration in a sub-tropical ridge-top cloud forest. J. Hydrol. 462-463, 42–52. https://doi.org/10.1016/j.jhydrol.2011.08.069.

García-Santos, G., Bruijnzeel, L.A., Dolman, A.J., 2009. Modelling canopy conductance under wet and dry conditions in a subtropical cloud forest. Agric. For. Meteorol. 149, 1565–1572. https://doi.org/10.1016/j.agrformet.2009.03.008.

Ghimire, C.P., Bruijnzeel, L.A., Lubczynski, M.W., Ravelona, M., Zwartendijk, B.W., van Meerveld, H.J., 2017. Measurement and modeling of rainfall interception by two differently aged secondary forests in upland eastern Madagascar. J. Hydrol. 545, 212–225. https://doi.org/10.1016/j.jhydrol.2016.10.032.

Ghimire, C.P., Bruijnzeel, L.A., Lubczynski, M.W., Zwartendijk, B.W., Odongo, V.O., Ravelona, M., van Meerveld, H.J., 2018. Transpiration and stomatal conductance in a young secondary tropical montane forest: contrasts between native trees and invasive understorey shrubs. Tree Physiol. 38 (7), 1053–1070. https://doi.org/10.1093/treephys/tpy004.

Ghimire, C.P., Lubczynski, M.W., Bruijnzeel, L.A., Chavarro-Rincón, D., 2014. Transpiration and canopy conductance of two contrasting forest types in the Lesser Himalaya of Central Nepal. Agric. For. Meteorol. 197, 76–90. https://doi.org/10.1016/j.agrformet.2014.05.012.

Giambelluca, T.W., 2002. Hydrology of altered tropical forest. Hydrol. Processes 16 (8), 1665–1669. https://doi.org/10.1002/hyp.5021.

Giambelluca, T.W., Fox, J., Yarnasarn, S., Onibutr, P., Nullet, M.A., 1999. Dry-season radiation balance of land covers replacing forest in northern Thailand. Agric. For. Meteorol. 95 (1), 53–65. https://doi.org/10.1016/S0168-1923(99)00016-7.

Giambelluca, T.W., Nullet, M.A., Ziegler, A.D., Tran, L., 2000. Latent and sensible energy flux over deforested land surfaces in the Eastern Amazon and Northern Thailand. Singap. J. Trop. Geogr. 21 (2), 107–130. https://doi.org/10.1111/1467-9493.00070.

Giambelluca, T.W., Ziegler, A.D., Nullet, M.A., Truong, D.M., Tran, L.T., 2003. Transpiration in a small tropical forest patch. Agric. For. Meteorol. 117 (1), 1–22. https://doi.org/10.1016/S0168-1923(03)00041-8.

Good, S.P., Noone, D., Bowen, G., 2015. Hydrologic connectivity constrains partitioning of global terrestrial water fluxes. Science 349 (6244), 175–177. https://doi.org/10.1126/science.aaa5931.

Granier, A., 1985. Une nouvelle méthode pour la mesure du flux de sève brute dans le tronc des arbres. Ann. For. Sci. 42 (2), 193–200. https://doi.org/10.1051/forest:19850204.

Granier, A., 1987. Evaluation of transpiration in a Douglas-fir stand by means of sap flow measurements. Tree Physiol. 3 (4), 309–320. https://doi.org/10.1093/treephys/3.4.309.

Granier, A., Biron, P., Bréda, N., Pontailler, J.-Y., Saugier, B., 1996. Transpiration of trees and forest stands: short and long-term monitoring using sapflow methods. Global Change Biol. 2 (3), 265–274. https://doi.org/10.1111/j.1365-2486.1996.tb00078.x.

Grissino-Mayer, H.D., 2003. A Manual and Tutorial for the Proper Use of an Increment Borer. Proc. Int. Meet. Stable Isot. Tree-Ring Res. 59 (2), 63–79.

Groemping, U., 2006. Relative importance for linear regression in R: The package Relaimpo 17(1), 27. doi:10.18637/jss.v017.i01.

Hardanto, A., Röll, A., Hendrayanto, Hölscher, D., 2017. Tree soil water uptake and transpiration in mono-cultural and jungle rubber stands of Sumatra. Forest Ecol. Manag. 397, 67–77. https://doi.org/10.1016/j.foreco.2017.04.032.

Heinimann, A., Mertz, O., Frolking, S., Egelund Christensen, A., Hurni, K., Sedano, F., Parsons Chini, L., Sahajpal, R., Hansen, M., Hurtt, G., 2017. A global view of shifting cultivation: recent, current, and future extent. PLoS One 12 (9), e0184479. https://doi.org/10.1371/journal.pone.0184479.

Hölscher, D., de, A., Sá, T.D., Bastos, T.X., Denich, M., Fölster, H., 1997. Evaporation from young secondary vegetation in eastern Amazonia. J. Hydrol. 193 (1), 293–305. https://doi.org/10.1016/S0022-1694(96)03145-9.

Hölscher, D., Köhler, L., Leuschner, C., Kappelle, M., 2003. Nutrient fluxes in stemflow and throughfall in three successional stages of an upper montane rain forest in Costa Rica. J. Trop. Ecol. 19 (5), 557–565. http://www.jstor.org/stable/4092003.

Hölscher, D., Sá, T.D., Möller, R.F., Denich, M., Fölster, H., 1998. Rainfall partitioning and related hydrochemical fluxes in a diverse and in a mono specific (Phenakospermum guyannense) secondary vegetation stand in eastern Amazonia. Oecologia 114 (2), 251–257. https://doi.org/10.1007/s004420050443.

Holwerda, F., Alvarado-Barrientos, M.S., González-Martínez, T.M., 2016. Surface energy exchange in a tropical montane cloud forest environment: Flux partitioning, and seasonal and land cover-related variations. Agric. For. Meteorol. 228-229, 13–28. https://doi.org/10.1016/j.agrformet.2016.06.011.

Horna, V., Schuldt, B., Brix, S., Leuschner, C., 2011. Environment and tree size controlling stem sap flux in a perhumid tropical forest of Central Sulawesi, Indonesia. Ann. Forest Sci. 68 (5), 1027–1038. https://doi.org/10.1007/s13595-011-0110-2.

Horning, N., Hewson, J., 2017. Very High Resolution Derived Land Cover/Use Classifications for the Corridor Ankeniheny-Zahamena (CAZ). Madagascar NERC Environmental Information Data Centre. https://doi.org/10.5285/ce535cef-842e-4875-ad80-26760900cec0.

Hu, Y., Zhao, P., Shen, W., Zhu, L., Ni, G., Zhao, X., Zhang, Z., Rao, X., Ouyang, L., Zeng, X., Sun, D., Lin, Y., 2018. Responses of tree transpiration and growth to seasonal rainfall redistribution in a subtropical evergreen broad-leaved forest. Ecosystems 21 (4), 811–826. https://doi.org/10.1007/s10021-017-0185-1.

Jackson, P.C., Cavelier, J., Goldstein, G., Meinzer, F.C., Holbrook, N.M., 1995. Partitioning of water resources among plants of a lowland tropical forest. Oecologia 101 (2), 197–203. https://doi.org/10.1007/BF00317284.

Jasechko, S., Sharp, Z.D., Gibson, J.J., Birks, S.J., Yi, Y., Fawcett, P.J., 2013. Terrestrial water fluxes dominated by transpiration. Nature 496 (7445), 347–350. https://doi.org/10.1038/nature11983.

Juhrbandt, J., Leuschner, C., Hölscher, D., 2004. The relationship between maximal stomatal conductance and leaf traits in eight Southeast Asian early successional tree species. Forest Ecol. Manag. 202 (1), 245–256. https://doi.org/10.1016/j.foreco.2004.07.021.

Koeniger, P., Marshall, J.D., Link, T., Mulch, A., 2011. An inexpensive, fast, and reliable method for vacuum extraction of soil and plant water for stable isotope analyses by mass spectrometry. Rapid Commun. Mass Spectrom. 25, 3041–3048. https://doi.org/10.1002/rcm.5198.

Kunert, N., Aparecido, L.M.T., Higuchi, N., Santos, J.d., Trumbore, S., 2015. Higher tree transpiration due to road-associated edge effects in a tropical moist lowland forest. Agric. For. Meteorol. 213, 183–192. https://doi.org/10.1016/j.agrformet.2015.06.009.

Kunert, N., Schwendenmann, L., Hölscher, D., 2010. Seasonal dynamics of tree sap flux and water use in nine species in Panamanian forest plantations. Agric. For. Meteorol. 150 (3), 411–419. https://doi.org/10.1016/j.agrformet.2010.01.006.

Kunert, N., Schwendenmann, L., Potvin, C., Hölscher, D., 2012. Tree diversity enhances tree transpiration in a Panamanian forest plantation. J. Appl. Ecol. 49 (1), 135–144. https://doi.org/10.1111/j.1365-2664.2011.02065.x.

Landwehr, J.M., Coplen, T.B., 2004. Line-conditioned excess: a new method for characterizing stable hydrogen and oxygen isotope ratios in hydrologic systems. In: International Conference on Isotopes in Environmental Studies Aquatic Forum. Monte-Carlo, Monaco.

Law, B.E., Falge, E., Gu, L., Baldocchi, D.D., Bakwin, P., Berbigier, P., Davis, K., Dolman, A.J., Falk, M., Fuentes, J.D., Goldstein, A., Granier, A., Grelle, A., Hollinger, D., Janssens, I.A., Jarvis, P., Jensen, N.O., Katul, G., Mahli, Y., Wofsy, S., 2002. Environmental controls over carbon dioxide and water vapor exchange of terrestrial vegetation. Agric. For. Meteorol. 113 (1), 97–120. https://doi.org/10.1016/S0168-1923(02)00104-1.

Li, P., Feng, Z., Xiao, C., Boudmyxay, K., Liu, Y., 2018. Detecting and mapping annual newly-burned plots (NBP) of swiddening using historical Landsat data in Montane Mainland Southeast Asia (MMSEA) during 1988–2016. J. Geogr. Sci. 28 (9), 1307–1328. https://doi.org/10.1007/s11442-018-1527-4.

Lion, M., Kosugi, Y., Takanashi, S., Noguchi, S., Itoh, M., Katsuyama, M., Matsuo, N., Shamsuddin, S.-A., 2017. Evapotranspiration and water source of a tropical rainforest in peninsular Malaysia. Hydrol. Processes 31 (24), 4338–4353. https://doi.org/10.1002/hyp.11360.

Lu, P., Müller, W.J., Chacko, E.K., 2000. Spatial variations in xylem sap flux density in the trunk of orchard-grown, mature mango trees under changing soil water conditions. Tree Physiol. 20 (10), 683–692. https://doi.org/10.1093/treephys/20.10.683.

Lubczynski, M.W., Chavarro-Rincon, D.C., Rossiter, D.G., 2017. Conductive sapwood area prediction from stem and canopy areas—allometric equations of Kalahari trees, Botswana. Ecohydrology 10 (6), e1856. https://doi.org/10.1002/eco.1856.

Luis, V.C., Jimenez, M.S., Morales, D., Kucera, J., Wieser, G., 2005. Canopy transpiration of Canary pine forest. Agric. For. Meteorol. 135, 117–123. https://doi.org/10.1016/j.agrformet.2014.05.012.

Macinnis-Ng, C.M.O., Flores, E.E., Müller, H., Schwendenmann, L., 2014. Throughfall and stemflow vary seasonally in different land-use types in a lower montane tropical region of Panama. Hydrol. Processes 28 (4), 2174–2184. https://doi.org/10.1002/hyp.9754.

Martín-Gómez, P., Barbeta, A., Voltas, J., Peñuelas, J., Dennis, K., Palacio, S., Dawson, T. E., Ferrio, J.P., 2015. Isotope-ratio infrared spectroscopy: a reliable tool for the investigation of plant-water sources? New Phytol. 207 (3), 914–927. https://doi.org/10.1111/nph.13376.

McJannet, D., Fitch, P., Disher, M., Wallace, J., 2007. Measurements of transpiration in four tropical rainforest types of north Queensland, Australia. Hydrol. Processes 21 (26), 3549–3564. https://doi.org/10.1002/hyp.6576.

Meinzer, F.C., Andrade, J.L., Goldstein, G., Holbrook, N.M., Cavelier, J., Wright, S.J., 1999. Partitioning of soil water among canopy trees in a seasonally dry tropical forest. Oecologia 121 (3), 293–301. https://doi.org/10.1007/s004420050931.

Mennekes, D., Rinderer, M., Seeger, S., Orlowski, N., 2021. Ecohydrological travel times derived from *in situ* stable water isotope measurements in trees during a semi-controlled pot experiment. Hydrol. Earth Syst. Sci. 25, 4513–4530. https://doi.org/10.5194/hess-25-4513-2021.

Moser, G., Hertel, D., Leuschner, C., 2007. Altitudinal change in LAI and stand leaf biomass in tropical montane forests: a transect study in ecuador and a pan-tropical meta-analysis. Ecosystems 10 (6), 924–935. http://www.jstor.org/stable/27823733.

Motzer, T., Munz, N., Küppers, M., Schmitt, D., Anhuf, D., 2005. Stomatal conductance, transpiration and sap flow of tropical montane rain forest trees in the southern Ecuadorian Andes. Tree Physiol. 25 (10), 1283–1293. https://doi.org/10.1093/treephys/25.10.1283.

Mukul, S.A., Herbohn, J., 2016. The impacts of shifting cultivation on secondary forests dynamics in tropics: a synthesis of the key findings and spatio temporal distribution of research. Environ. Sci. Policy 55, 167–177. https://doi.org/10.1016/j.envsci.2015.10.005.

Muñoz-Villers, L.E., Holwerda, F., Alvarado-Barrientos, M.S., Geissert, D.R., Dawson, T. E., 2018. Reduced dry season transpiration is coupled with shallow soil water use in tropical montane forest trees. Oecologia 188 (1), 303–317. https://doi.org/10.1007/s00442-018-4209-0.

Nadezhdina, N., Čermák, J., Ceulemans, R., 2002. Radial patterns of sap flow in woody stems of dominant and understory species: scaling errors associated with positioning of sensors. Tree Physiol. 22 (13), 907–918. https://doi.org/10.1093/treephys/22.13.907.

Nehemy, M.F., Benettin, P., Allen, S.T., Steppe, K., Rinaldo, A., Lehmann, M.M., McDonnell, J.J., 2022. Phloem water isotopically different to xylem water: Potential causes and implications for ecohydrological tracing. Echohydrology 15, e2417. https://doi.org/10.1002/eco.2417.

Nepstad, D.C., Moutinho, P., Dias-Filho, M.B., Davidson, E., Cardinot, G., Markewitz, D., Figueiredo, R., Vianna, N., Chambers, J., Ray, D., Guerreiros, J.B., Lefebvre, P., Sternberg, L., Moreira, M., Barros, L., Ishida, F.Y., Tohlver, I., Belk, E., Kalif, K., Schwalbe, K., 2002. The effects of partial throughfall exclusion on canopy processes, aboveground production, and biogeochemistry of an Amazon forest. J. Geophys. Res. 107 (D20) https://doi.org/10.1029/2001JD000360. LBA 53-51-LBA 53-18.

O'Grady, A.P., Eamus, D., Hutley, L.B., 1999. Transpiration increases during the dry season: patterns of tree water use in eucalypt open-forests of northern Australia. Tree Physiol. 19 (9), 591–597. https://doi.org/10.1093/treephys/19.9.591.

Oliveira, R.S., Dawson, T.E., Burgess, S.S.O., Nepstad, D.C., 2005. Hydraulic redistribution in three Amazonian trees. Oecologia 145 (3), 354–363. https://doi.org/10.1007/s00442-005-0108-2.

Orlowski, N., Breuer, L., 2020. Sampling soil water along the pF curve for δ2H and δ18O analysis. Hydrol. Processes 34 (25), 4959–4972. https://doi.org/10.1002/hyp.13916.

Orlowski, N., Breuer, L., McDonnell, J.J., 2016. Critical issues with cryogenic extraction of soil water for stable isotope analysis. Ecohydrology 9 (1), 1–5. https://doi.org/10.1002/eco.1722.

Orlowski, N., Winkler, A., McDonnell, J.J., Breuer, L., 2018. A simple greenhouse experiment to explore the effect of cryogenic water extraction for tracing plant source water. Ecohydrology 11 (5), e1967. https://doi.org/10.1002/eco.1967.

Peng, S.-S., Piao, S., Zeng, Z., Ciais, P., Zhou, L., Li, L.Z.X., Myneni, R.B., Yin, Y., Zeng, H., 2014. Afforestation in China cools local land surface temperature. Proc. Natl. Acad. Sci. 111 (8), 2915–2919. https://doi.org/10.1073/pnas.1315126111.

Penna, D., Hopp, L., Scandellari, F., Allen, S.T., Benettin, P., Beyer, M., Geris, J., Klaus, J., Marshall, J.D., Schwendenmann, L., Volkmann, T.H.M., von Freyberg, J., Amin, A., Ceperley, N., Engel, M., Frentress, J., Giambastiani, Y., McDonnell, J.J., Zuecco, G., Kirchner, J.W., 2018. Ideas and perspectives: Tracing terrestrial ecosystem water fluxes using hydrogen and oxygen stable isotopes – challenges and opportunities from an interdisciplinary perspective. Biogeosciences 15 (21), 6399–6415. https://doi.org/10.5194/bg-15-6399-2018.

Peters, R.L., Fonti, P., Frank, D.C., Poyatos, R., Pappas, C., Kahmen, A., Carraro, V., Prendin, A.L., Schneider, L., Baltzer, J.L., Baron-Gafford, G.A., Dietrich, L., Heinrich, I., Minor, R.L., Sonnentag, O., Matheny, A.M., Wightman, M.G., Steppe, K., 2018. Quantification of uncertainties in conifer sap flow measured with the thermal dissipation method. New Phytol. 219, 1283–1299. https://doi.org/10.1111/nph.15241.

Phillips, D.L., Gregg, J.W., 2003. Source partitioning using stable isotopes: coping with too many sources. Oecologia 136, 261–269.

Pineda-García, F., Paz, H., Meinzer, F.C., 2013. Drought resistance in early and late secondary successional species from a tropical dry forest: the interplay between xylem resistance to embolism, sapwood water storage and leaf shedding. Plant Cell Environ. 36 (2), 405–418. https://doi.org/10.1111/j.1365-3040.2012.02582.x.

Poyatos, R., Čermák, J., Llorens, P., 2007. Variation in the radial patterns of sap flux density in pubescent oak (Quercus pubescens) and its implications for tree and stand transpiration measurements. Tree Physiol. 27 (4), 537–548. https://doi.org/10.1093/treephys/27.4.537.

Querejeta, J.I., Estrada-Medina, H., Allen, M.F., Jiménez-Osornio, J.J., 2007. Water source partitioning among trees growing on shallow karst soils in a seasonally dry tropical climate. Oecologia 152 (1), 26–36. https://doi.org/10.1007/s00442-006-0629-3.

Querejeta, J.I., Estrada-Medina, H., Allen, M.F., Jiménez-Osornio, J.J., Ruenes, R., 2006. Utilization of bedrock water by Brosimum alicastrum trees growing on shallow soil atop limestone in a dry tropical climate. Plant Soil 287 (1), 187. https://doi.org/10.1007/s11104-006-9065-8.

R Development Core Team, 2011. R: a Language and Environment for Statistical Computing. R Foundation for Statistical Computing, Vienna, Austria.

Razakamanarivo, H., Razafimbelo, T., Andriamananjara, A., Rianahary, A., Razafindrakoto, M., Harinirina, A., 2017. Soil profile and chemistry data in the Ankeniheny Zahamena forest corridor, Madagascar NERC Environmental Information Data Centre. doi:10.5285/c3884aa0-b083-469d-8a0d-fdbbb79aff05.

Reyes-Acosta, J.L., Lubczynski, M.W., 2014. Optimization of dry-season sap flow measurements in an oak semi-arid open woodland in Spain. Ecohydrology 7 (2), 258–277. https://doi.org/10.1002/eco.1339.

Roberts, S., Vertessy, R., Grayson, R., 2001. Transpiration from Eucalyptus sieberi (L. Johnson) forests of different age. Forest Ecol. Manag. 143 (1), 153–161. https://doi.org/10.1016/S0378-1127(00)00514-4.

Rothfuss, Y., Javaux, M., 2017. Reviews and syntheses: Isotopic approaches to quantify root water uptake: a review and comparison of methods. Biogeosciences 14, 2199–2224. https://doi.org/10.5194/bg-14-2199-2017.

Rust, S., 1999. Comparison of three methods for determining the conductive xylem area of Scots pine (Pinus sylvestris). Forestry 72 (2), 103–108. https://doi.org/10.1093/forestry/72.2.103.

Schaap, M.G., Leij, F.J., van Genuchten, M.T.H., 2001. ROSETTA: a computer program for estimating soil hydraulic parameters with hierarchical pedotransfer functions. J. Hydrol. 251, 163–176. https://doi.org/10.1016/S0022-1694(01)00466-8.

Schlesinger, W.H., Jasechko, S., 2014. Transpiration in the global water cycle. Agric. For. Meteorol. 189-190, 115–117. https://doi.org/10.1016/j.agrformet.2014.01.011.

Schwendenmann, L., Pendall, E., Sanchez-Bragado, R., Kunert, N., Hölscher, D., 2015. Tree water uptake in a tropical plantation varying in tree diversity: interspecific differences, seasonal shifts and complementarity. Ecohydrology 8 (1), 1–12. https://doi.org/10.1002/eco.1479.

Schwendenmann, L., Veldkamp, E., Moser, G., Hölscher, D., Köhler, M., Clough, Y., Anas, I., Djajakirana, G., Erasmi, S., Hertel, D., Leitner, D., Leuschner, C., Michalzik, B., Propastin, P., Tjoa, A., Tscharntke, T., Van Straaten, O., 2010. Effects of an experimental drought on the functioning of a cacao agroforestry system, Sulawesi, Indonesia. Global Change Biol. 16 (5), 1515–1530. https://doi.org/10.1111/j.1365-2486.2009.02034.x.

Sinacore, K., Asbjornsen, H., Hernandez-Santana, V., Hall, J.S., 2019. Drought differentially affects growth, transpiration, and water use efficiency of mixed and monospecific planted forests. Forests 10 (2), 153. https://www.mdpi.com/1999-4907/10/2/153.

Sinacore, K., Hall, J.S., Potvin, C., Royo, A.A., Ducey, M.J., Ashton, M.S., 2017. Unearthing the hidden world of roots: Root biomass and architecture differ among species within the same guild. PLoS One 12 (10), e0185934. https://doi.org/10.1371/journal.pone.0185934.

Sohel, M.S.I., Grau, A.V., McDonnell, J.J., Herbohn, J., 2021. Tropical forest water source patterns revealed by stable isotopes: a preliminary analysis of 46 neighboring species. Forest Ecol. Manag. 494, 119355 https://doi.org/10.1016/j.foreco.2021.119355.

Sommer, R., Fölster, H., Vielhauer, K., Carvalho, E.J.M., Vlek, P.L.G., 2003. Deep soil water dynamics and depletion by secondary vegetation in the Eastern Amazon. Soil Sci. Soc. Am. J. 67 (6), 1672–1686. https://doi.org/10.2136/sssaj2003.1672.

Sommer, R., Sá, T.D.d.A., Vielhauer, K., Araújo, A.C.d., Fölster, H., Vlek, P.L.G., 2002. Transpiration and canopy conductance of secondary vegetation in the eastern Amazon. Agric. For. Meteorol. 112 (2), 103–121. https://doi.org/10.1016/S0168-1923(02)00044-8.

Sprenger, M., Allen, S.T., 2020. What ecohydrologic separation is and where we can go with it. Water Resour. Res. 56 (7), e2020WR027238 https://doi.org/10.1029/2020WR027238.

Sprenger, M., Llorens, P., Cayuela, C., Gallart, F., Latron, J., 2019. Mechanisms of consistently disjunct soil water pools over (pore) space and time. Hydrol. Earth Syst. Sci. 23 (6), 2751–2762. https://doi.org/10.5194/hess-23-2751-2019.

Stahl, C., Hérault, B., Rossi, V., Burban, B., Bréchet, C., Bonal, D., 2013. Depth of soil water uptake by tropical rainforest trees during dry periods: does tree dimension matter? Oecologia 173 (4), 1191–1201. https://doi.org/10.1007/s00442-013-2724-6.

Stock, B.C., Jackson, A.L., Ward, E.J., Parnell, A.C., Phillips, D.L., Semmens, B.X., 2018. Analyzing mixing systems using a new generation of Bayesian tracer mixing models. PeerJ 6, e5096. https://doi.org/10.7717/peerj.5096.

Stock, B. C., Semmens, B. X., 2016. "MixSIAR GUI user manual." doi: 10.5281/zenodo.1209993, Version 3.1, https://github.com/brianstock/MixSIAR.

Styger, E., Rakotondramasy, H.M., Pfeffer, M.J., Fernandes, E.C.M., Bates, D.M., 2007. Influence of slash-and-burn farming practices on fallow succession and land degradation in the rainforest region of Madagascar. Agric. Ecosyst. Environ. 119 (3), 257–269. https://doi.org/10.1016/j.agee.2006.07.012.

Tanaka, K., Takizawa, H., Tanaka, N., Kosaka, I., Yoschifuji, N., Tantasirin, C., Piman, S., Suzuki, M, Tangtham, N., 2003. Transpiration peak over a hill evergreen forest in northern Thailand in the late dry season: assessing the seasonal changes in evapotranspiration using a multilayer model. J. Geophys. Res. 108 (D17) https://doi.org/10.1029/2002JD003028.

Turc, L., 1961. Estimation of irrigation water requirements, potential evapotranspiration: A simple climatic formula evolved up to date. Ann. Agron. 12, 13–49.

van der Tol, C., 2012. Validation of remote sensing of bare soil ground heat flux. Remote Sens. Environ. 121, 275–286. https://doi.org/10.1016/j.rse.2012.02.009.

van Meerveld, H.J., Jones, J.P.G., Ghimire, C.P., Zwartendijk, B.W., Lahitiana, J., Ravelona, M., Mulligan, M., 2021. Forest regeneration can positively contribute to local hydrological ecosystem services: Implications for forest landscape restoration. J. Appl. Ecol. 58, 755–765. https://doi.org/10.1111/1365-2664.13836.

van Vliet, N., Mertz, O., Heinimann, A., Langanke, T., Pascual, U., Schmook, B., Adams, C., Schmidt-Vogt, D., Messerli, P., Leisz, S., Castella, J.-C., Jørgensen, L.,

Birch-Thomsen, T., Hett, C., Bech-Bruun, T., Ickowitz, A., Vu, K.C., Yasuyuki, K., Fox, J., Ziegler, A.D., 2012. Trends, drivers and impacts of changes in Swidden cultivation in tropical forest-agriculture frontiers: a global assessment. Glob. Environ. Chang. 22 (2), 418–429. https://doi.org/10.1016/j.gloenvcha.2011.10.009.

Vertessy, R.A., Watson, F.G.R., O'Sullivan, S.K., 2001. Factors determining relations between stand age and catchment water balance in mountain ash forests. Forest Ecol. Manag. 143 (1), 13–26. https://doi.org/10.1016/S0378-1127(00)00501-6.

von Freyberg, J., Allen, S.T., Grossiord, C., Dawson, T.E., 2020. Plant and root-zone water isotopes are difficult to measure, explain, and predict: some practical recommendations for determining plant water sources. Methods Ecol. Evol. 11, 1352–1367. https://doi.org/10.1111/2041-210X.13461.

Von Randow, R.C.S., Rodriguez, D.A., Tomasella, J., Aguiar, A.P.D., Kruijt, B., Kabat, P., 2019. Response of the river discharge in the Tocantins River Basin, Brazil, to environmental changes and the associated effects on the energy potential. Region. Environ. Change 19 (1), 193–204. https://doi.org/10.1007/s10113-018-1396-5.

von Randow, R.d.C.S., Tomasella, J., von Randow, C., de Araújo, A.C., Manzi, A.O., Hutjes, R., Kruijt, B., 2020. Evapotranspiration and gross primary productivity of secondary vegetation in Amazonia inferred by eddy covariance. Agric. For. Meteorol. 294, 108141 https://doi.org/10.1016/j.agrformet.2020.108141.

Waterloo, M.J., Bruijnzeel, L.A., Vugts, H.F., Rawaqa, T.T., 1999. Evaporation from Pinus caribaea plantations on former grassland soils under maritime tropical conditions. Water Resour. Res. 35 (7), 2133–2144. https://doi.org/10.1029/1999WR900006.

Zimmermann, B., Zimmermann, A., Scheckenbach, H.L., Schmid, T., Hall, J.S., van Breugel, M., 2013. Changes in rainfall interception along a secondary forest succession gradient in lowland Panama. Hydrol. Earth Syst. Sci. 17 (11), 4659–4670. https://doi.org/10.5194/hess-17-4659-2013.

Zuecco, G., Amin, A., Frentress, J., Engle, M., Marchina, C., Anfodillo, T., Morga, M., Carraro, V., Scandellari, F., Tagliavini, M., Zanotelli, D., Comiti, F., Penna, D., 2020. A comparative study of plant water extraction methods for isotopic analyses: Scholander-type pressure chamber vs. cryogenic vacuum distillation. Hydrology and Earth System Sciences Discussion [preprint], in review. doi:10.5194/hess-2020-446.

Bretfeld, M., Ewers, B.E., Hall, J.S., Ogden, F.L., 2015. Sapflow-based transpiration estimates in species-rich secondary forests of different ages in Central Panama during a wet-season drought. American Geophysical Union Fall Meeting December 2015, poster H4313–1494.

Zwartendijk, B.W., et al., 2020. Soil water- and overland flow dynamics in a tropical catchment subject to long-term slash-and-burn agriculture. J. Hydrol. 582, 124287 https://doi.org/10.1016/j.jhydrol.2019.124287.